

UNIVERSITY OF MINNESOTA

This is to certify that I have examined this copy of a master's thesis by

Darrick Donald Zarling

and have found that it is complete and satisfactory in all respects,
and that any and all revisions required by the final
examining committee have been made.

David B. Kittelson
Name of Faculty Advisor

Signature of Faculty Advisor

Date

GRADUATE SCHOOL

HIGH SPEED CYCLE RESOLVED SAMPLING OF THE EXHAUST
FROM A DIRECT INJECTION DIESEL ENGINE

A THESIS
SUBMITTED TO THE FACULTY OF THE GRADUATE SCHOOL
OF THE UNIVERSITY OF MINNESOTA
BY

Darrick Donald Zarling

IN PARTIAL FULFILLMENT OF THE REQUIREMENTS
FOR THE DEGREE OF
MASTER OF SCIENCE

DECEMBER, 1997

Acknowledgments

I would like to gratefully acknowledge and thank the many companies involved for donating money, equipment and/or time in support of the research conducted for this thesis. These companies included John Deere, Exxon, and General Motors.

I would also like to thank the faculty, students, and staff, especially D. B. Kittelson, E. A. Fletcher, Michael Pipho, Imad Abdul-Khalek, and Betsy Antinozzi, along with many others who have supported me throughout my career at the University of Minnesota.

Finally, I would like to thank my family for their continued support and patience through this long process. Without them, none of this would have been possible.

Abstract

A system that allows collection and analysis of the exhaust from individual engine cycles has been built. Its development and performance are described. The system was used to study the cyclic variability of a 0.7 liter diesel cylinder operating at 1500 rpm and an equivalence ratio of 0.6. The cyclic variability of particulate mass emissions associated with in-cylinder processes was found to be 40% of the mean. The variability of NO_x emissions that could be associated with in-cylinder processes was much lower, only 6% of the mean. The variability of pressure development in the combustion process was very low, less than 2% of the mean. The high variability of particulate emissions may be due to high sensitivity of the formation/oxidation balance to small changes in the combustion process, to in-cylinder surface deposition/resuspension processes, or to some combination of the two. Of course other unidentified phenomena may play a role.

Table of Contents

1. INTRODUCTION IV

2. BACKGROUND 3

3. APPARATUS & PROCEDURE..... 6

A. INTRODUCTION 6

B. THE SAMPLER 6

Objective..... 6

Constraints..... 8

Implementation 11

C. ENGINE & HYDRAULIC DRIVE SYSTEM..... 22

D. INSTRUMENTS AND MEASUREMENT SYSTEMS 29

High Speed Data Acquisition System..... 29

Dilution Tunnel..... 30

Gas Analyzers 30

Particle Measurement Systems 31

E. TEST PROCEDURE 33

Steady State..... 33

Single Cycle 34

4. RESULTS & DISCUSSION..... 37

A. SAMPLING SYSTEM PERFORMANCE 37

Speed of Response 37

Leakage, Particle Losses, and Resuspension..... 39

Procedure to Minimize Sampling Artifacts..... 44

B. SINGLE CYCLE MEASUREMENTS..... 45

C. STEADY STATE MEASUREMENTS 52

D. DISCUSSION OF SINGLE CYCLE TESTS..... 52

5. CONCLUSIONS & RECOMMENDATIONS 56

BIBLIOGRAPHY 58

APPENDIX 1: SUMMARIZED DATA 60

APPENDIX 2: T-TEST RESULTS 61

List of Figures

| | |
|--|----|
| Figure 3.1 - Sampling System Block Diagram..... | 8 |
| Figure 3.2 - Engine Operating Timeline..... | 11 |
| Figure 3.3 - Alternative Valve Designs..... | 13 |
| Figure 3.4 - Basic Sampler Elements | 14 |
| Figure 3.5 - Test Setup Schematic..... | 16 |
| Figure 3.6 - Arrangement of Sliding Valve, Actuator, and Backing Plate..... | 18 |
| Figure 3.7 - Sampling Valve and Associated Systems Schematic | 20 |
| Figure 3.8 - Nitrogen Purge Manifold..... | 23 |
| Figure 3.9 - Longitudinal and Cross Section View of 4JB1 Engine | 26 |
| Figure 3.10 - Schematic of Hydraulic Drive System..... | 27 |
| Figure 3-11 - Dilution Tunnel System | 33 |
| Figure 3.12 - Single Cycle Sampling Apparatus | 37 |
| Figure 4.1 - Sample Valve Motion and Cylinder Pressure..... | 39 |
| Figure 4.2 - Total Particle Mass Emissions..... | 49 |
| Figure 4.3 - Coefficients of Variation for Single Cycle Sampler Measurements..... | 50 |
| Figure 4.4 - Cumulative Frequency Distributions for Single Cycle Measurements..... | 56 |

List of Tables

| | |
|--|----|
| Table 1.1: Federal Diesel Truck Emissions Standards..... | 2 |
| Table 3.1: Preliminary Response Time Tests..... | 17 |
| Table 3.2: Engine Specifications..... | 24 |
| Table 4.1: Initial System Check Results | 42 |
| Table 4.2: Resuspension Testing Results | 44 |
| Table 4.3: Non-fired Testing Results | 44 |
| Table 4.4: Summary Of Measurements..... | 47 |
| Table 4.5: Brake Specific Emissions..... | 50 |
| Table 4.6: Correlation Coefficients..... | 54 |

1. INTRODUCTION

It is becoming increasingly difficult to meet ever decreasing diesel exhaust emission standards. Table 1.1 lists the EPA emissions standards timetable for new heavy-duty highway trucks. In order to produce cleaner engines, in-cylinder processes must be understood in great detail. Phenomena that were unrecognized or considered unimportant may now be responsible for a significant fraction of the exhaust emissions. Insights into some of the phenomena may be gained through the use of advanced diagnostic techniques including spatially and temporally resolved exhaust measurements. This thesis focuses on cycle resolved exhaust measurements.

| Year | HC | NO _x | CO | PM |
|------|-----|-----------------|------|------|
| 1990 | 1.3 | 6.0 | 15.5 | 0.6 |
| 1991 | 1.3 | 5.0 | 15.5 | 0.25 |
| 1994 | 1.3 | 5.0 | 15.5 | 0.1 |
| 1998 | 1.3 | 4.0 | 15.5 | 0.1 |

It is well established that spark ignition engines have significant cycle-to-cycle variability in flame travel and pressure development. On the other hand, diesel engines show little variability in pressure development. The objective of this study was to determine if this cyclic consistency also applies to NO_x and particulate emissions. This was done by building and testing a system for cycle resolved exhaust sampling and using it to characterize a representative diesel engine.

If emissions vary significantly from cycle-to-cycle, one must ask why. Are there wall interactions? Is the charge motion different? Is the residual fraction different? If

the variability is on the order of the emission standards, a control strategy might be to minimize the high emission cycles and maximize the low cycles. This study does not attempt to answer such questions. Its purpose is to establish the degree of cyclic variability of emissions in order to determine if they are worth asking. This is done with a newly designed and built sample valve which will allow the exhaust from one cycle of one cylinder to be collected for subsequent analysis. The samples collected in this study are a combination of two cycles. The port volume from the previous cycle is pushed into the sample line ahead of the exhaust pulse from the cycle of interest. The volume of the port was estimated to be between 0.07 and 0.1 liters. The displacement volume of the cylinder is 0.693 liters. That leads to about 10 to 12 % of the exhaust volume collected being from the previous cycle and the same percent of the desired exhaust being lost. As this is an initial study, testing was done at only one engine operating condition, 1500 rpm with an equivalence ratio of 0.6.

This work is also an extension of the Total Cylinder Sampling (dumping) experiments which have been underway at the University of Minnesota since the early 80's. The difficulty of conducting those experiments made performing enough tests to determine variability from cycle-to-cycle an almost impossibility. Those tests consisted of a series of samples collected at different times during the combustion event, each sample of a different cycle. The variation from cycle-to-cycle would be an additional tool to gain additional insights into the data collected in those experiments.

2. Background

Diesel engine particles are the result of a global three step process, formation, growth, and oxidation. It has been shown that a significant portion of the particles formed are oxidized within the cylinder before the exhaust process commences.^{18,19,20} Recent studies have shown that a large fraction of the emitted particles have been in contact with in-cylinder surfaces.^{8,9,21}

The cyclic variability in spark ignition engines has been studied extensively.^{18,19} This variability is shown to have a significant affect on many combustion variables leading to a large variability in the emissions on a cycle resolved basis. The variability can often be related to variability present in the combustion process as indicated by the pressure development in the cylinder.

Only a few previous studies have attempted to examine the cyclic variability of exhaust emissions from diesel engines. Stenerson¹ used basically the same sampler to study exhaust emission variations on a John Deere direct injection diesel engine and found a significant cycle-to-cycle variability in NO_x and particulate emissions. Xu et al.² used a light scattering method to measure in-cylinder particle concentrations. They found that average scattering intensities correlated well with a readings from a Bosch smoke meter. They also observed that exhaust scattering intensities varied significantly from cycle-to-cycle. At 75% load they found a 3.5:1 range in the scattering intensity. This suggests significant cyclic variability of particle emissions. Ferguson, et al.³ measured the exhaust particle concentrations using a light attenuation method. They found that the cycle-to-cycle variations were negligible except near the smoke limit. However, the

optical attenuation method that they used may not have been sufficiently sensitive to detect variability at lighter loads. Kittelson and Collings⁴ found that the response of an electrostatic probe inserted into the exhaust of an indirect injection diesel engine could be related to average exhaust particle mass concentration. They observed significant cycle-to-cycle variations in the probe signal. They suggested that this might be due to cyclic variability in resuspension of particles from in-cylinder and exhaust port surfaces.

Many in-cylinder studies of pollutant formation in diesel engines have been performed. The results of several of these studies suggest significant cycle-to-cycle differences in in-cylinder particle concentrations. Xu et al.² found significant cycle-to-cycle variation in light scattering from a small jet issuing from the combustion chamber of a direct injection diesel engine. Total cylinder sampling experiments performed at the University of Minnesota with both indirect and direct injection diesel engines have shown significant difference in particle mass concentrations measured at essentially the same crankangle during different engine cycles^{5,6}. These differences were attributed to cyclic variability in particle formation and oxidation. Yan and Borman⁷ measured in-cylinder radiation and temperature. They observed significant cycle-to-cycle differences in in-cylinder radiation. They show a 2.5:1 range in the normalized radiation signals. They found no correlation between the cyclic signal and changes in the injection process. Tree and Foster²⁰ used two optical methods, which involved light scattering, extinction and radiation to measure soot particle size, number density, and temperature. They note that there is large cycle-to-cycle variation in the early and late parts of the cycle although no quantitative measurements are given.

Cyclic variation in exhaust particle concentration may result not only from inconstancies in in-cylinder formation and oxidation processes, but also from surface interactions. This was suggested in the work of Kittelson and Collings.⁴ The importance of wall interactions has been established in several recent studies. Kittelson et al.⁸ suggest that significant quantities of particulate matter are deposited on in-cylinder surfaces by thermophoresis, the movement of particles down a temperature gradient. This material is later resuspended by charge motion during the exhaust stroke. They suggest that as much as 50% of the particulate matter emitted has interacted with the walls. Abukdais⁹ did time averaged, crankangle resolved measurements of particle concentration and size in the exhaust of an indirect injection diesel engine. He found that particle concentrations were higher and particles were larger during the early blowdown phase than in the later displacement phase of the exhaust stroke. He attributed this to resuspension of particles deposited on the walls during combustion by the high velocities present during exhaust blowdown.

The studies described above suggest that there may be significant variability in formation and emission of particulate matter by diesel engines. However, only one other direct measurement of the cyclic variability of emitted particulate mass has been made.¹ The main objective of the work described here is to make cycle resolved particle mass measurements. The sampling system was designed so that cycle resolved measurements of gaseous species, especially NO_x, also could be made.

3. Apparatus & Procedure

A. Introduction

In order to meet the objective of the thesis, to make cycle resolved particle mass measurements, a single cycle sampling valve was designed, built, integrated into the existing system, and tested. This system was installed on a 2.8 liter direct injection Isuzu diesel engine described in detail by Takeuchi et al.¹⁶ In this section the design objectives and constraints, the design implementation, and the performance of the final design are described.

B. The Sampler

Objective

The single cycle sampling valve must divert the exhaust flow from the standard exhaust line into the sample bag and then return the exhaust flow to the standard line over the period of one engine cycle. The design of the sample system must connect the engine with both a standard exhaust line and the sample bag and be able to switch the exhaust flow from one to the other. The following block diagram, figure 3.1, illustrates the concept. Many of the components are already in place, including the engine, tunnel control valves, and the sample bag.

The design for the sampler resulted from looking at a large variety of possibilities, from the exotic to the very simple, and trying to pick one that would function well and remain relatively uncomplicated. An example of a more exotic type design is a valve used by

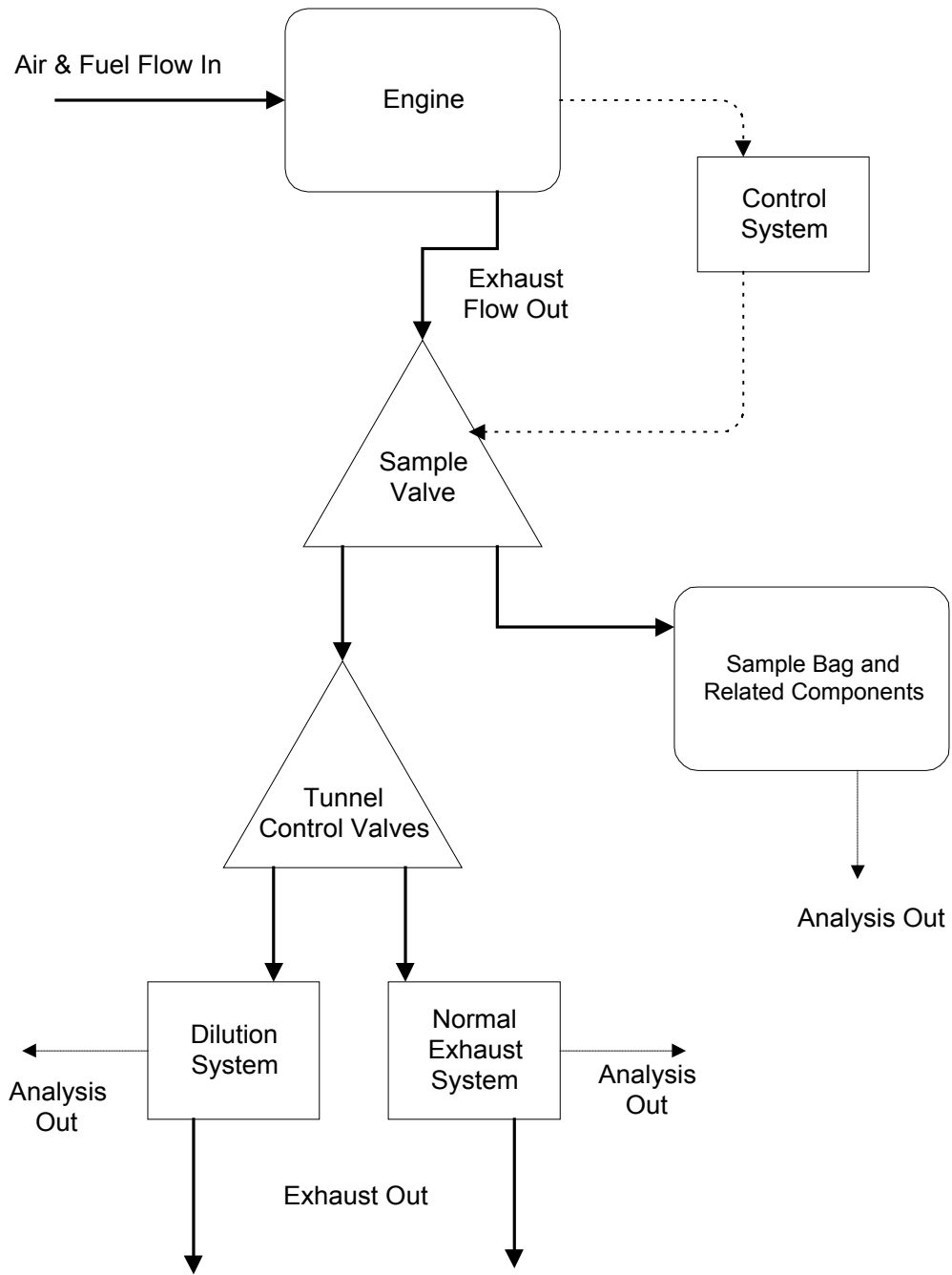


Figure 3.1 - Sampling System Block Diagram

General Motors Research Laboratories¹⁷ to switch the engine air flow from intake to exhaust on a single valve research engine. This valve was operated continuously to perform its task. The major problem with this valve or a similar design is sealing. A simple valve would be a standard industrial three-way valve. Such a valve was used to direct the engine exhaust between the tunnel and the normal exhaust path. It did not survive well in the harsh environment of diesel exhaust and began to leak. It was also large, heavy, and difficult to move from one position to the other.

Constraints

An ideal system would capture and quench all the exhaust from one engine cycle with no leakage, particle loss, particle reentrainment, or contamination and allow for the analysis of the combustion products. The system would allow repeated samples to be acquired without interfering with normal operation of the engine. To further define the design of the valve, a list of constraints was developed. The primary constraints were:

1. Speed. The valve must move fast enough to complete its travel between successive exhaust strokes while the engine exhaust valve is closed. Many of the tests performed on this engine have been done at 1500 rpm. Consequently, this was taken as the minimum speed requirement. At 1500 rpm the exhaust valve is open for approximately 20 ms and closed for approximately 60 ms. Thus, the sampling valve would have to complete its travel in less than 60 ms. A fast response actuator and low effective inertia of the moving parts are required to achieve this. An engine

operation timeline, figure 3.2, is useful to define the necessary speed and accuracy with which the valve must move. The valve must move within certain time slots defined by when the exhaust valve is closed.

2. Sealing. Sealing integrity must be maintained while still allowing rapid motion. The valve should not allow leakage from the exhaust into the sampling system while the engine is operating or leakage out of the sampling system. Slight leakage out of the exhaust line while the engine is operating normally is not a major concern. A moving seal is required so the sealing system must have low friction and good wear characteristics.
3. Thermal Resistance. The valve and seals must be able to withstand temperatures ranging from the temperature of the coolant, 80 -120 °C, to the highest exhaust temperatures, about 400 °C for this engine.
4. Dead Volume. The valve mechanism must be mounted as close as possible to the exhaust port on the cylinder head to minimize the volume between the engine exhaust valve and the sampling valve. The exhaust trapped in this volume is left over from the previous cycle and reduces the resolution of the sampling system.
5. Accurate sampling. The sample must not be altered significantly by the sampling process. Thus wall losses must be minimized. In addition, care must be taken to

avoid resuspension of particulate matter from sampling system surfaces. Adequate quenching and diluting of the exhaust is also necessary for accurate analysis of the collected sample.

6. Cost. The sampling system must be relatively simple and constructed from low cost, easily available materials in a reasonable amount of time.

7. Compatibility. The new sampler must be compatible with as many existing systems as possible. It must fit into an allowable area defined by the engine and provide a link between the engine and the sampling system without major modifications to either system component.

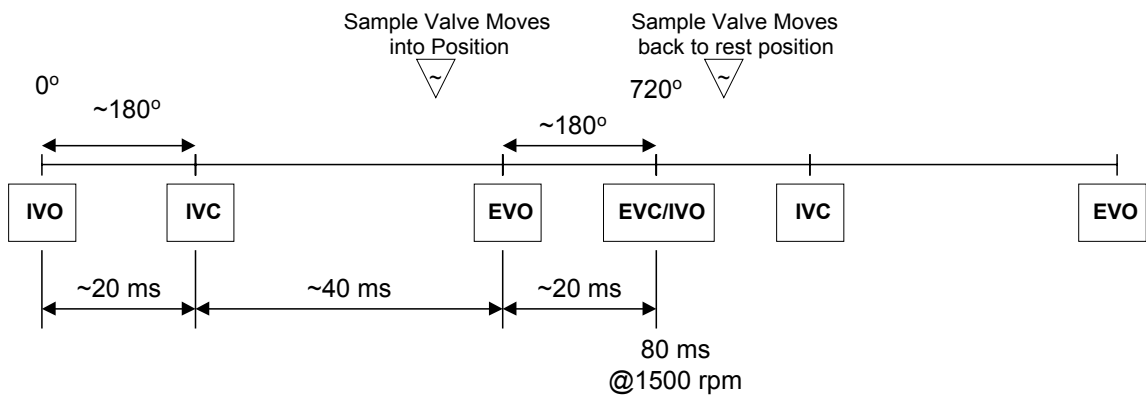


Figure 3.2 - Engine Operating Timeline

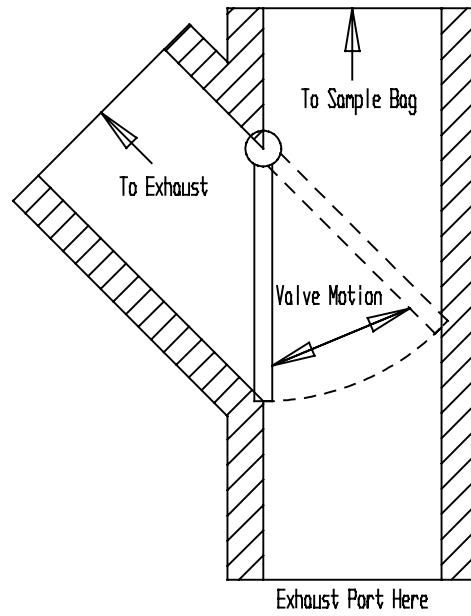
(IVO / IVC = intake valve open / close, EVO / EVC = exhaust open / close)

Implementation

After careful consideration of all the design objectives and constraints two candidates: a "Y-pipe" type valve and a "sliding" type valve mechanism were both given further consideration. They are illustrated in figure 3.3. Either type valve would offer advantages. A Y-pipe, more attractive in many ways, would be difficult to seal, especially under the conditions present in the exhaust. Side seals such as those used in rotary engines were considered but would prove difficult to fabricate. A Y-pipe type valve as shown in figure 3.3 would have minimal inertia of the valve components and offer a very direct sample path. It could also be designed to connect to the engine in a small area. The volume of the Y-pipe valve would likely be larger than that of a sliding type valve as a sample line would be connected to the valve further from the exhaust port. The sliding type valve as shown in an overhead view in figure 3.3 would offer close access to the exhaust port and likely minimize any contamination of the sample line during normal operation as the sample port would be isolated from the exhaust port. It would require moving a larger mass, but not so large as to be a major concern. After considering these factors, the sliding system was chosen because we could not devise a low cost design of an effective seal for the Y-pipe system whereas there were no obvious insurmountable design hurdles with a sliding type valve.

A sliding type system could consist of any number of different variations. Two specific types reviewed were a pure slide, where the whole valve moves linearly, and a design with a pivot point that the valve would slide around. A design with linear travel

Y Type Valve



Sliding Type Valve

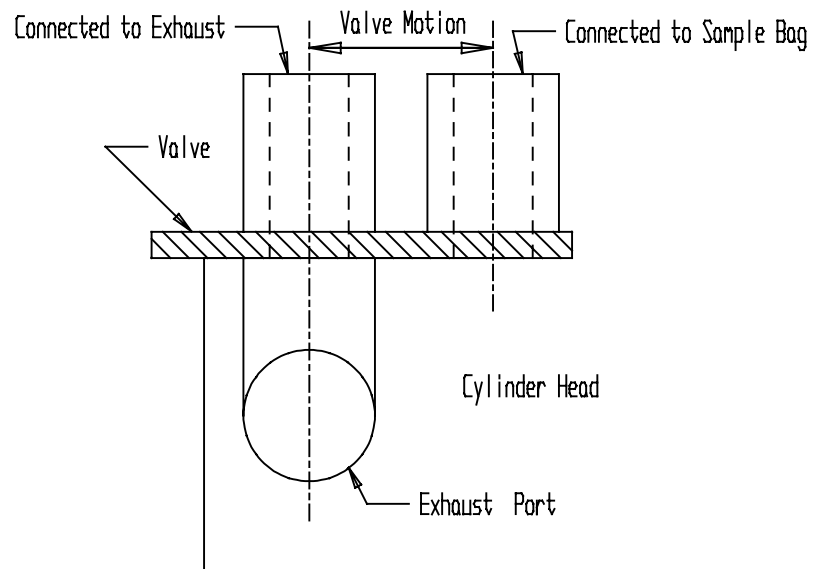


Figure 3.3 - Alternative Valve Designs

would be difficult to keep in line without very exact guides. A pivot point, along with a single actuation point would minimize such issue. In order to maintain alignment integrity and allow for ease of fabrication, a design with a pivot point was chosen.

The basic elements of the sampling valve are shown in figure 3.4. The valve itself is a rotating, sliding mechanism consisting of two primary pieces; a stationary base plate which is attached directly to the engine and a slider plate rides on the base plate.

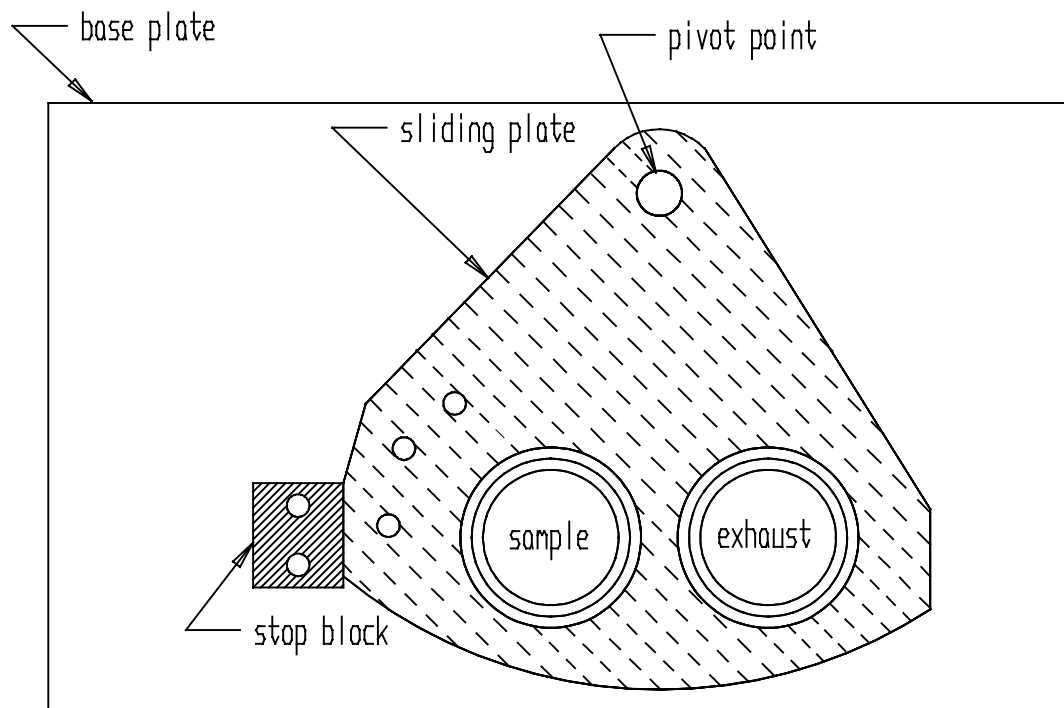


Figure 3.4 - Basic Sampler Elements

Electric, hydraulic, and pneumatic systems were considered for valve actuation. Hydraulic systems appeared to be too complicated. A hydraulic pump and reservoir would be required, along with more expensive valve and control systems as compared to other options. Hydraulic actuators tend to be heavy, and have somewhat longer response times. The response times of electro-mechanical actuators, linear or rotary solenoids, were such that it would be difficult to find an electric system that would move such a sampler rapidly enough. They are also limited in travel and output force. A pneumatic system, however, looked as if it would do the job very well. The laboratory is equipped with air lines and the related components, pneumatic cylinders and solenoid control valves, are readily available at reasonable cost. Fast acting solenoid valves and light weight, quick response cylinders are available. This type system was chosen for the initial trials. A pneumatic cylinder and solenoid control valves already available in the laboratory was selected for preliminary testing.

Feasibility tests were run to verify that a pneumatic actuator could provide the required forces and response times. A Clippard Mini-Matic 18 D-3, 1.125 inch bore x 8.5 inch stroke, double acting pneumatic cylinder controlled by two Clippard solenoid valves model 2021 ET-3M-12 was used. It was mounted vertically so that rates of lifting several different weights could be determined. A test schematic is shown in figure 3.5. A MTI KD320 Fotonic Sensor fiber-optic position sensor and digital oscilloscope were used to time the system. The fiber-optic sensor transmits light with half the fiber bundle and receives light with the other half. A special reflective tape is used as reflect light back to the sensor. The sensor give a voltage output proportional to the received light. When the

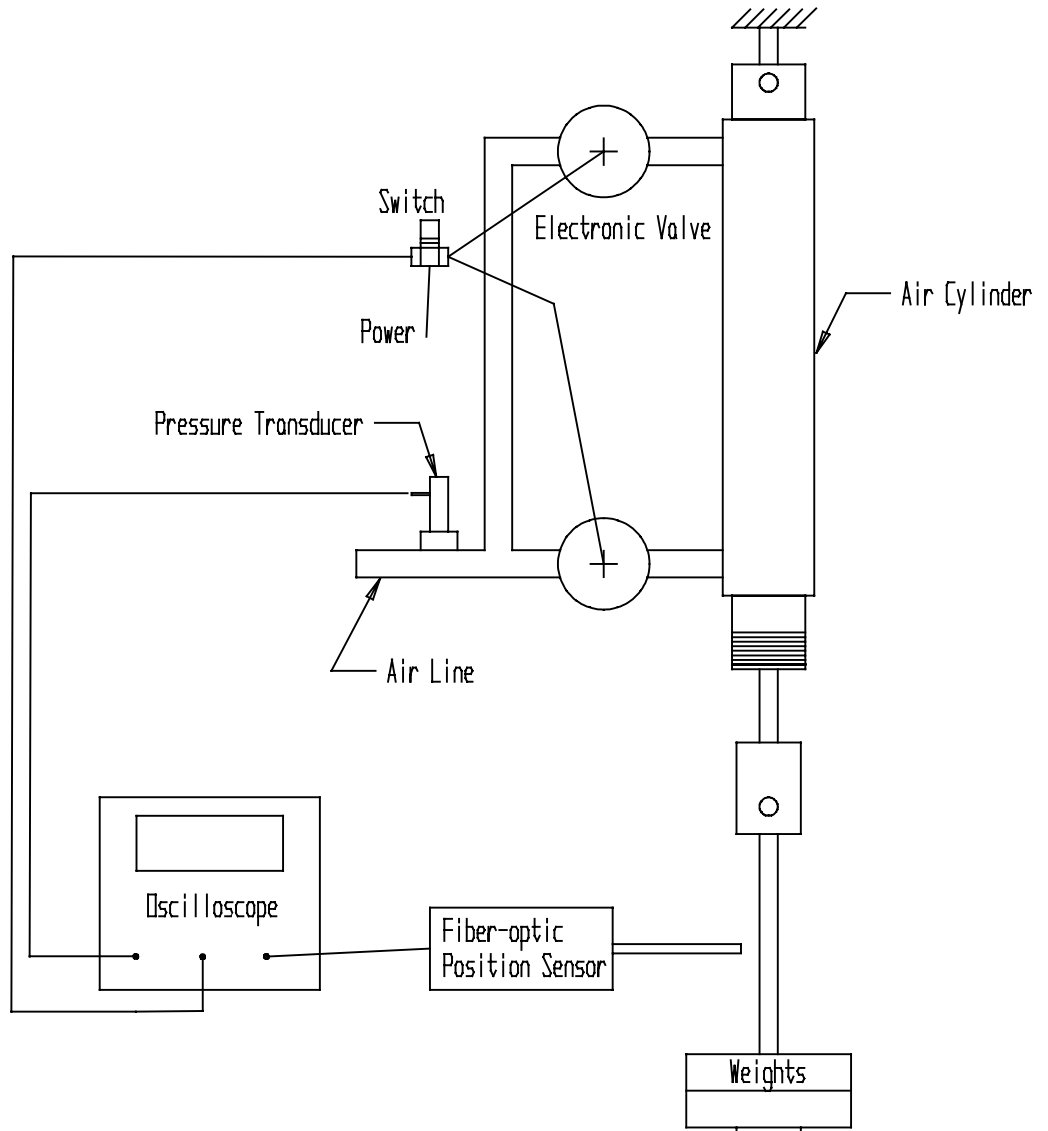


Figure 3.5 - Test Setup Schematic

tape is placed only in the specific locations the position of the weight hanger, in this case, can be determined. It was also fitted with a pressure transducer to determine the delay between signal activation and solenoid valve opening. The test results in table 3.1 show the move time, the time required to fully retract the cylinder, and delay time, the time delay between sending the signal and actual cylinder movement.

| Table 3.1: Preliminary Response Time Tests (move time, delay time (ms)) | | |
|--|-------------------------|--------------------------|
| Weight (lb.) | 75 psig supply pressure | 100 psig supply pressure |
| 0.65 | 17,-- | -- |
| 1.9 | 26,19 | -- |
| 3.15 | 36,16 | 31,19 |

The results of this simple test show it is possible to actuate an air cylinder through its stroke moving a reasonably heavy weight in the times required. Move times have to be less than 60 ms with the engine operating at 1500 rpm. The delay will not be a problem as long as it remains constant. It will have to be taken into account in the control system and monitored to assure consistency. The move command will have to be sent approximately 20 ms, or 180 CAD before the cylinder needs to start moving.

Based on this testing a double acting pneumatic cylinder was chosen to actuate the valve shown in figure 3.4. The basic elements of the sample valve are shown in figure 3.6.

The sampler is moved with an air cylinder that is electronically controlled. The control system consists of an encoder mounted on the engine, a set of timers, and process electronics which actuate two two-way solenoid valves, one to extend the cylinder and one to retract it. A two-way fiber-optic sensor is used to verify the position of the slider.

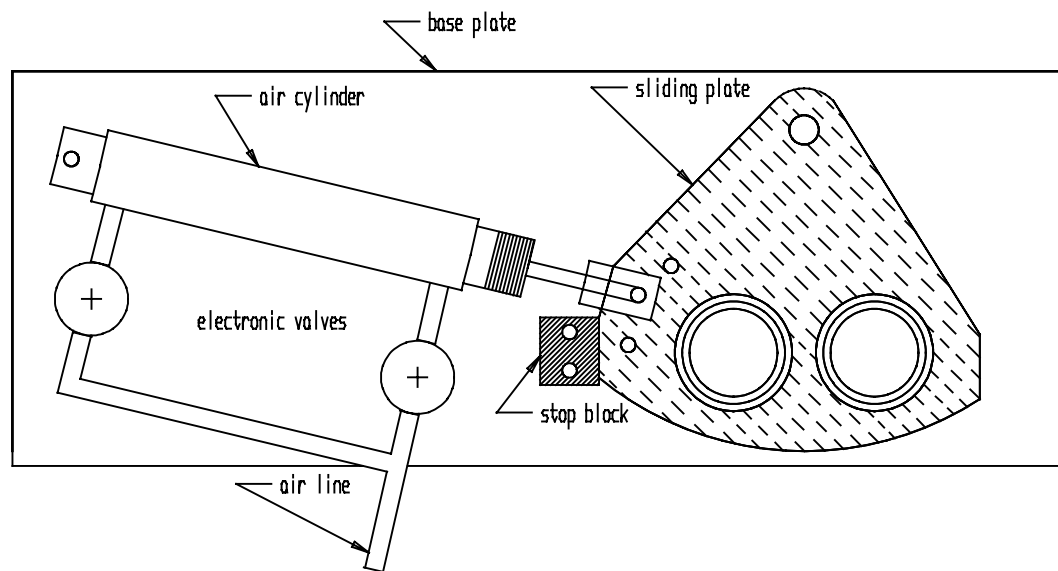


Figure 3.6 - Arrangement of Sliding Valve, Actuator, and Backing Plate

The sampler works by allowing exhaust to flow normally out through port A and then switching the flow to port B while the exhaust valve is closed as shown in figure 3.7. Then the sampler allows the exhaust from a single cycle flow into a sampling bag. Once the exhaust valve closes the sample moves back to it's original position so the exhaust again may flow out though port A.

The test results showed that it would be possible to build a sampler based on pneumatic actuation. The next step in the sampler design was to select appropriate tubing to connect the sampler to the exhaust line and to the sample bag. Various flexible and rotating (solid pipe connections with rotating seals at the ends) designs were considered including polymeric and flexible metal lines. In the required size range the polymeric

tubing was not flexible and would not have adequate thermal resistance. Many of the more exotic polymers were not available in the sizes needed. Light weight, flexibility, and low particle losses were primary considerations. Flexible corrugated stainless steel was selected. This type of connector was the only available alternative that would withstand exhaust temperatures while maintaining flexibility. Particle losses were examined and are discussed below along with overall system performance.

In the final design flexible corrugated stainless steel tubes (Superflex from TC Hose) are used to connect the movable slider to the stationary exhaust line and to the sample bag as shown in figure 3.7.

Sealing was the last major design problem to be overcome. Teflon o-rings are mounted in the back side of the slider in order to provide a seal so that exhaust gases do not leak or contaminate the sample line. Teflon o-rings were also used to seal the flange on the SS flexible tubing and the mounting post on the slider. This allows the end of the flexible tubing to rotate at the valve connection as the valve moves and be fixed on the other end. The entire slider is held to the base plate by three springs, one located on the pivot post and two located on the hold down clamp which acts on the lower edge of the slider. The hold down clamp consists of an aluminum plate over a Teflon plate which rides on the slider. At the pivot point Teflon shims are used to level the plate. Teflon is used throughout this system due to its ability to withstand the temperatures along with its slipperiness and inertness. Although the exhaust gases may reach 400 °C and Teflon can only withstand about 260 °C the seals seem to hold up. Apparently, this is because the engine coolant is maintained at 82 °C so that most of the sampler system remains at a

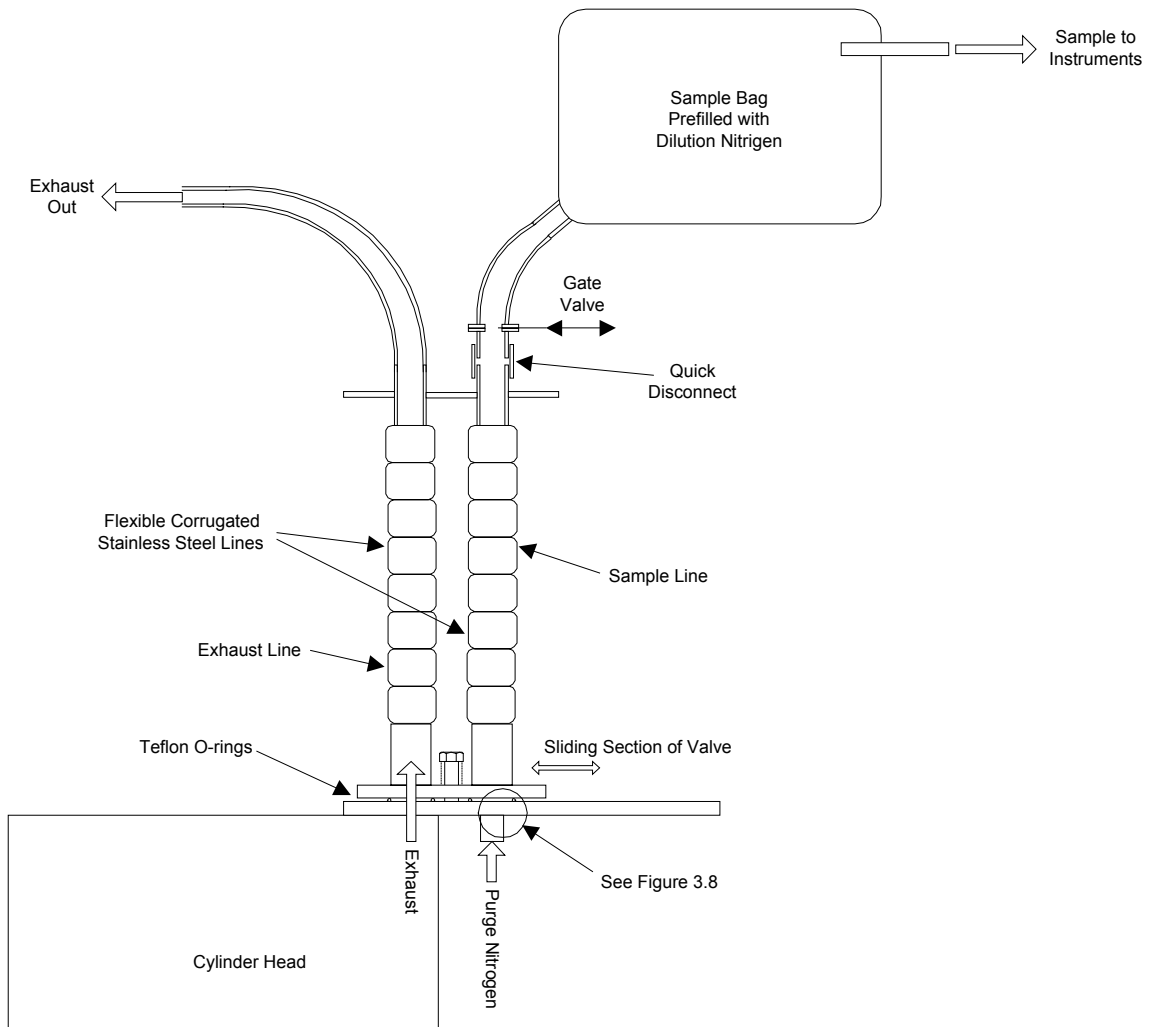


Figure 3.7 - Sampling Valve and Associated Systems Schematic

temperature much below that of the exhaust stream. A thermocouple placed between the engine head and the standard fixed exhaust manifold measured the temperature to be 193 °C during normal steady state operation. By blowing room temperature air over the manifold this temperature was reduced to 110 °C. This procedure was not implemented for the testing reported on which follows but could be useful at other operating conditions or when testing a different engine

One shortcoming of the system is that the samples collected in this study are a combination of two cycles. The port volume from the previous cycle is pushed into the sample line ahead of the exhaust pulse from the cycle of interest. The volume of the port was estimated to be between 0.07 and 0.1 liters. The displacement volume of the cylinder is 0.693 liters. That leads to about 10 to 12 % of the exhaust volume collected being from the previous cycle and the same percent of the desired exhaust being lost. From the thesis of Abukdais⁸ it can be seen that the particle mass in the last 10 percent of the exhaust emitted is of a considerably smaller fraction, maybe about 5%.

In order to minimize particle deposition and resuspension, the flow path from the exhaust valve to the sampling system was made as direct and short as possible. Roughness, cracks, and crevices were avoided. Deposition and resuspension and other potential sampling errors were examined carefully and are described in some detail below.

In order to minimize cost, the system was designed to be compatible with as many existing systems as possible. The engine used for these experiments was already set up

for the in-cylinder sampling experiments.^{6,10} Some elements of the control system, the sample collection system, and most of the instrumentation were shared with the in-cylinder sampling apparatus.

In order to time the sampler with the engine it was connected to the existing set of timers which are driven by the shaft encoder. The timers change state at a predetermined crankangle setting which triggers the valves that operate the air cylinder through interface electronics. The experiment controller and interface electronics are further described in the following sections.

A purge gas system was added to the sampling system to force all the collected exhaust from the sample line into the sample bag as shown in figure 3.7, 3.8, and 3.12. Figure 3.8 shows a cutout section of the baseplate indicating the orifice plate, manifold, and nitrogen connection used for the purge system. This is done with a small nitrogen cylinder that was a part of the existing test apparatus. The cylinder is pre-filled with N₂ and emptied into the line at the appropriate time with a solenoid valve connected to one of the experiment controller's available timers. The timer was set to discharge the N₂ into the sample line as soon as the sampler returned to the rest position to minimize particle settling in the sample line.

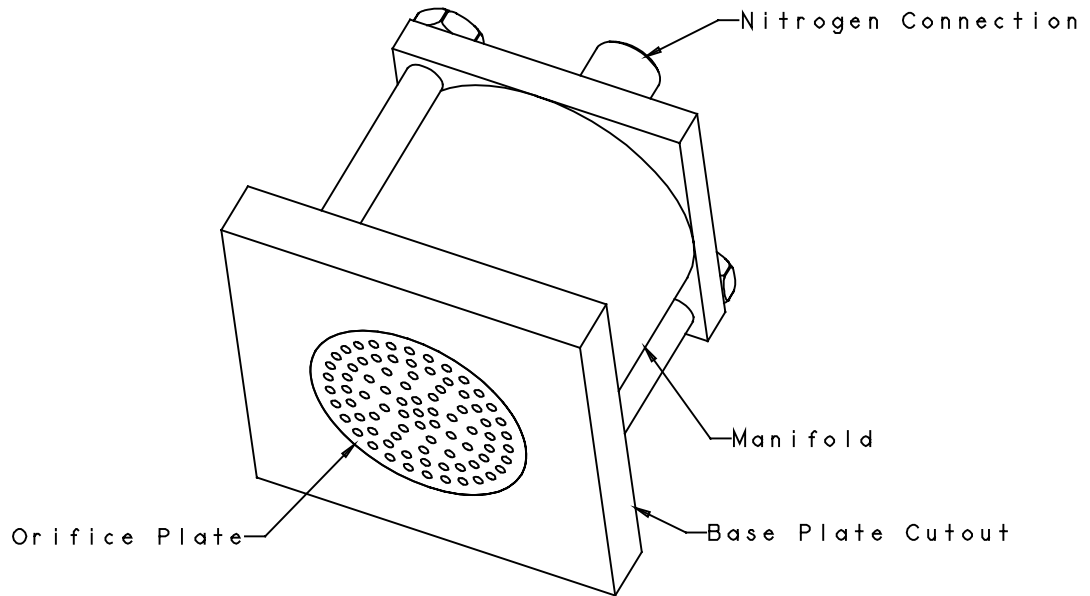


Figure 3.8 - Nitrogen Purge Manifold

C. Engine & Hydraulic Drive System

The test engine is an Isuzu 2.8 liter model 4JB1 four cylinder direct injection diesel engine. Engine specifications are given in table 3.2. Cross-sectional views of the engine are shown in figure 3.9¹⁶. The engine was previously modified to allow single cylinder operation with only cylinder number four remaining operational. This cylinder has isolated intake and exhaust manifolds. The three extra injectors inject into a chamber where the pressure is regulated at 4.8 MPa. This fuel is recirculated to the injection pump and allows for normal operation of the fuel injection system. The injector line has been

fitted with a pressure transducer and the injector has a needle lift sensor. The engine coolant temperature is controlled externally and is maintained at 82 °C.

| | |
|-----------------------|----------------------------|
| Bore | 93 mm |
| Stroke | 102 mm |
| Connecting Rod Length | 169 mm |
| Piston Bowl | Squared with reentrant lip |
| Injection System | Bosch VE type |
| Injector Holes | 4 @0.28 mm diam |
| Injection Pressure | 18.1 MPa |
| Compression Ratio | 18.6 |

As the engine was modified to have only one functioning cylinder, for most conditions additional power is required to drive the engine. This is accomplished with a hydraulic pump/motor combination. A schematic of the hydraulic system is show in figure 3.8. The system consists of an Eaton Model 54 variable displacement hydraulic pump, an Eaton Model 33 fixed displacement hydraulic motor, and a Detroit Diesel 453 turbocharged diesel engine. The pump speed is controlled by a Fenner M-Trim digital controller through a Moog Model 62-512B servo control valve. The controller receives speed information from an encoder mounted on the engine. The controller is able to maintain engine speed within ± 2 RPM and can also ramp engine speed up or down.

The engine systems are essentially the same as those used in the total cylinder sampling experiments described by Kittelson et al.⁶ and Pipho¹⁰.

The engine has been equipped with the appropriate instrumentation to allow for the control and monitoring of the operating parameters.

Temperature Measurements

Standard type K thermocouples have been installed to measure engine coolant, oil, intake air, and fuel temperatures. The thermocouples are read by an Omega 650 thermocouple display through a manual selector switch. Temperature is measured at the air inlet, fuel inlet, engine oil, and coolant inlet and outlet.

Air Flow Measurements

The air flow to the number four cylinder is measured with a Meriam Model 50MW20-2 laminar flow element and a Dwyer Magnehelic type gauge with a range of 10 cm H₂O. A type K thermocouple measures upstream temperature. An air cleaner is used to clean the incoming air. Factory calibration curves are used to calculate the air flow from the measure pressure drop and temperature.

Fuel Flow Measurements

The fuel flow is monitored using a Brooks Micro Oval, oval gear type flowmeter. The flowmeter outputs a signal for each revolution of a particular gear, indicating volume flow rate. Mass flow rate was then determined using a spreadsheet based on measured calibration curves with the inputs of counts, time and fuel temperature.

Figure 3.9 - Longitudinal and Cross Section View of 4JB1 Engine

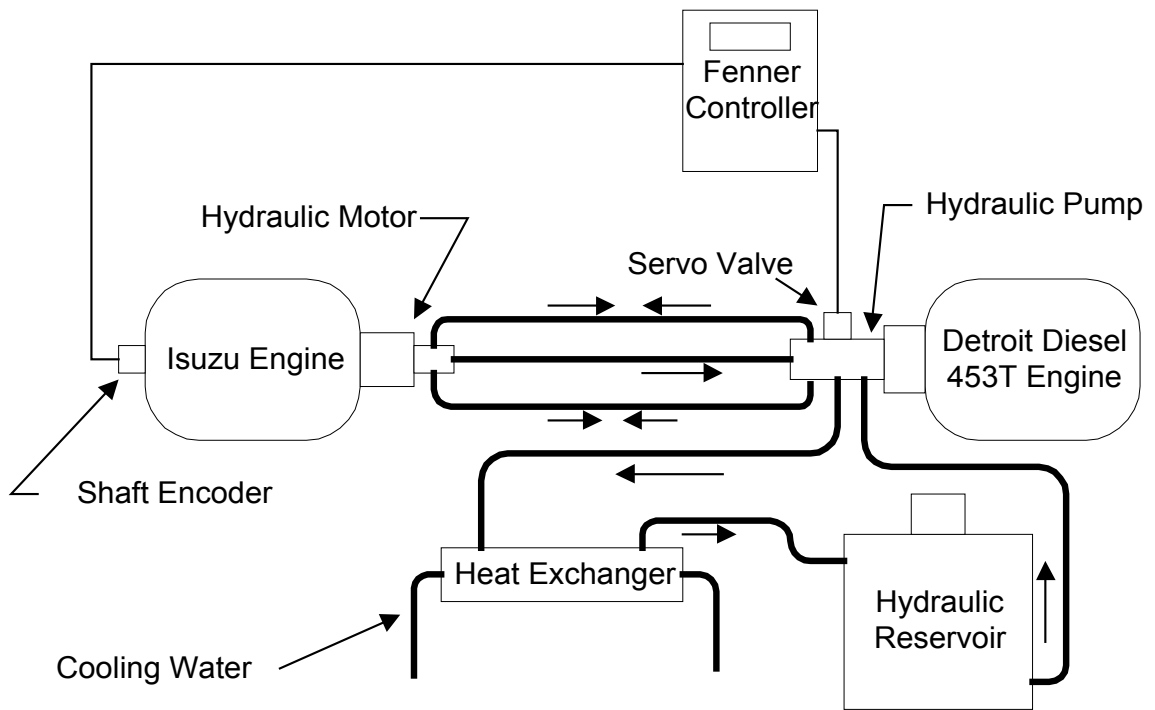


Figure 3.10 - Schematic of Hydraulic Drive System

Cylinder Pressure Measurements

Cylinder pressure is measured with an AVL 8QP water cooled pressure transducer which was mounted flush with the combustion chamber surface. The charge output from the transducer was fed to a Kistler model 504 amplifier which provides a voltage output for the data acquisition system. A dead weight tester, in conjunction with the data acquisition system, was used to calibrate the pressure transducer. Calibration was typically performed if the transducer was removed from the engine for any reason or if there was any problem with the sensor output.

Needle Lift Measurements

The operating injector has been fitted with a Wolff Hall Effect displacement transducer that is used as a needle lift sensor. The output is fed through a differential amplifier to the data acquisition system. This sensor is used to determine start of injection and injection duration.

Injection Line Pressure

The fuel line pressure is measured with a Kistler Model 596 pressure transducer. The signal is sent through a Kistler Model 504 amplifier to the data acquisition system.

Flame Luminosity Measurements

Flame luminosity is monitored with a Dolan Jenner model 7150 photodiode viewing the combustion chamber through an infrared filter and a fiber optic bundle. The filter allows only infrared light to reach the sensor, which is mounted above the valve cover and fed by the fiber optic bundle. The fiber optic bundle is installed vertically between the intake and exhaust valves. A quartz window protected the end of the bundle

which was cleaned with isopropyl alcohol when the signal deteriorated. The output of the photodiode sensor is input to a Dolan Jenner Micro Optic II series 8230 control system which has been modified by General Motors Research Laboratories to provide an analog output signal. Despite the limitations of the sensor, which include narrow viewing angle and a strong temperature dependence, an attempt was made to correlate the output with that of other measured sensor outputs.

Crankshaft Position Measurements

A Trump Ross rotary encoder was coupled to the front of the crankshaft. The encoder allows the engine speed and crankangle position to be monitored. The encoder provides two TTL logic level signals, a 0.5 crank angle degree (CAD) signal once per revolution which was aligned with top dead center of cylinder number four and a square wave with a period of one CAD. These signals were sent to the data acquisition and experiment control systems.

Experiment Controller

An experiment controller is used to generate event signals based on preset engine CAD settings. The controller consists of four identical counter-comparator systems which are able to provide an output signal at any of the 720 crankangle degrees in a four stroke cycle. The desired setpoint is adjusted using thumbwheel switches on the controller. The cylinder pressure was used by the system to ensure that the timers were synchronized with TDC of the compression stroke of cylinder number four.¹⁰ The system output was a 10 volt signal.

An optically coupled interface circuit was built in order to provide a digital trigger for the new sampler. Two 4N32 Photo-Darlington Opto-Isolators were used for isolation. The opto-isolators drive 74121 monostable multivibrators which in turn trigger a latching flip-flop built from a single 7400 Quadruple 2-input positive-nand gate chip. Three flip-flops were wired with the third input being a manual switch used to de-energize both solenoids. The circuit control the solenoids through two 511 power MOSFETs which switch the +12V solenoid power supply. The interface circuit itself is powered by a +5V supply.

D. Instruments and Measurement Systems

High Speed Data Acquisition System

A Nicollet 4094 digital oscilloscope is used to acquire the data from the test engine. The system was identical to that described by Pipho.¹⁰ Cylinder pressure, TDC, injector needle lift, in-cylinder luminosity, sampler position were all captured real time by the oscilloscope. The oscilloscope took data synchronously with the engine using the crankshaft encoder output to initiate each data point collection. Once stored in the oscilloscope memory the data was downloaded to a personal computer via a GPIB port using PRES-ANAL, a program written by Pipho.¹⁰ The program is capable of calculating several relative parameters and plotting the data. The data can also be stored for future analysis.

Dilution Tunnel

The dilution tunnel, shown in figure 3.9, is used to take the exhaust measurements. It is made of 3 inch ID aluminum tubing arranged in a C-shape due to space limitations. The dilution air is provided by a Dresser Industries Model 2510J roots blower. Approximately 270 moles of dilution air per minute is supplied by the roots blower. The air is filtered and flow is measured using an orifice. The exhaust from cylinder number four is injected into the tunnel in a counter flow direction. After the exhaust flow is injected, there is a 1.5 m mixing section and then the flow splits into two parts with 800 lpm flowing into the sampling section and the remainder piped outside. The 800 lpm flow is controlled by a Sierra Model 350 high volume sampler. A sample line is fitted to the wall of the tunnel just prior to the end. Dilution ratios of 12 to 25 are provided depending on the engine exhaust and dilution flows. The dilution ratio, D, is defined as;

$$D = \frac{\text{Exhaust Flow} + \text{Dilution Flow}}{\text{Exhaust Flow}}$$

D is determined by measurement of the dilution flow and the engine inlet flow which is then corrected for the decrease of molecular weight through the engine.¹⁰

Exhaust flow to the tunnel is controlled by two 1.5 inch gate valves. The exhaust from cylinder number four can either be sent to the tunnel or diverted outside the building.

Gas Analyzers

CO₂ and NO_x concentration were measured in undiluted exhaust for the steady state tests. All measurements made using the single cycle sampler were made on dilute samples. A Thermo Electron Model 10A chemiluminescent NO_x analyzer was used to

measure NO and NO₂ concentrations in the undiluted exhaust, and a high sensitivity Monitor Labs Model 8840 chemiluminescent NO_x analyzer was used to measure the NO and NO₂ in the dilute samples. A Beckman Model 215B Infrared analyzer with 5.25 and 0.125 inch long sample cells was used to measure CO₂ concentrations. The short cell was used for the undiluted exhaust samples and the long cell was used for the dilute samples.

The analyzers were calibrated with a zero gas and the appropriate range of span gas at startup and at the end of use for a given set of samples. All lab personnel were familiar with the procedure.

Particle Measurement Systems

All particle measurements were made on diluted samples. The full flow dilution tunnels shown in figure 3.7 was used for steady state measurements. In the single cycle measurements, the samples were diluted with nitrogen as they entered the sample bag. Particle mass and size distribution measurements were made using a Micro Orifice Uniform Deposition Impactor (MOUDI).¹¹ The total mass collected by the single cycle sampler was very small, usually less than 100 µg. This made it difficult to collect enough mass on individual impactor stage for accurate weighing. Consequently the MOUDI was operated with only one impactor stage and a backup filter. A 1.0 µm impactor stage was used for the preliminary experiments. A 10 µm stage was used for the main series of experiments along with the 1 µm stage. In all cases 37 mm Pallflex TX40HI20WW Teflon coated glass fiber backup filters were used.

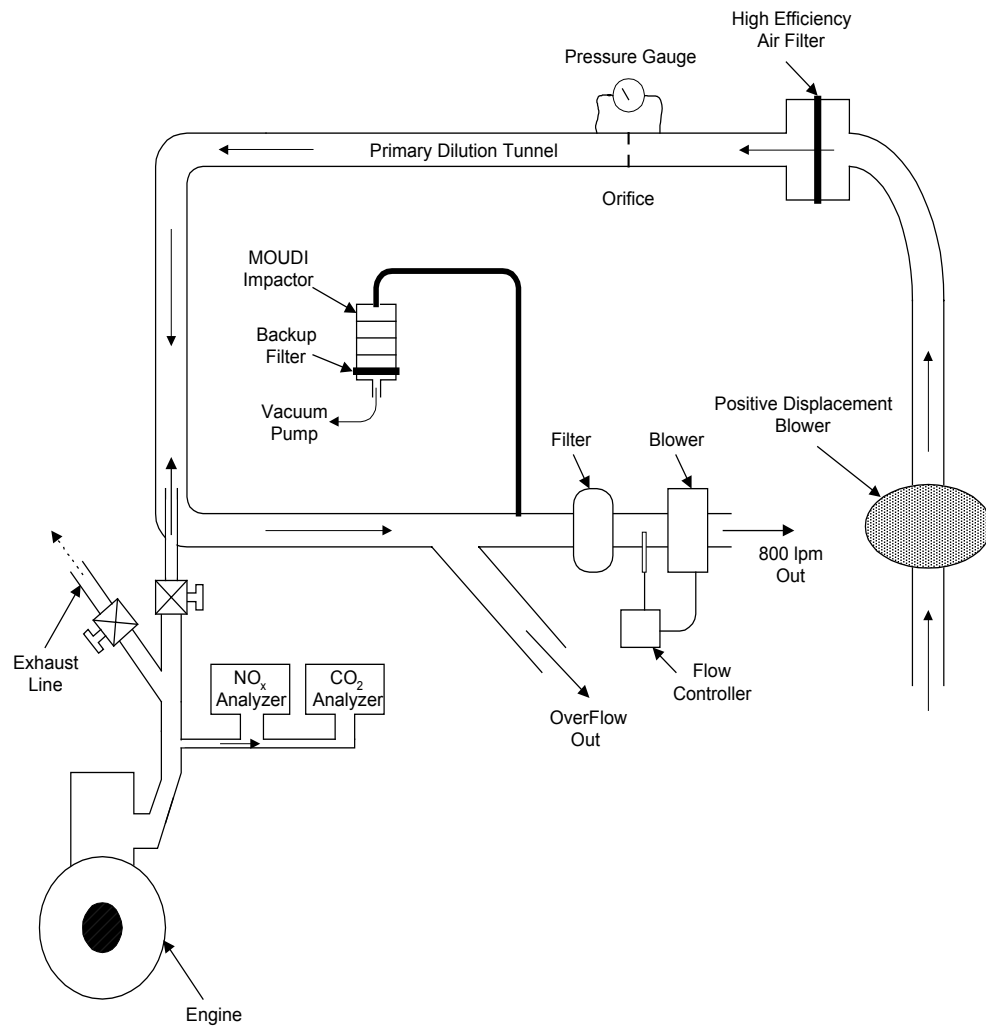


Figure 3-11 - Dilution Tunnel System

E. Test Procedure

The first step in the procedure is preparation of the filters and foils. This is done as described by Piphro¹⁰ and Rubow¹². The filters were baked at 230 °C for 24 hours and then allowed to equilibrate in the weighing room another 24 hours. The average temperature and humidity in the weighing room were 23 °C and 48 %, respectively, when weighing was conducted for this thesis. The impactor foils have a silicone spray applied to them and then were baked at 66 °C for 90 min. They were then allowed to equilibrate overnight before weighing. This process leaves a stable, sticky film on the surface of the foils that prevents particle bounce. The foils and filters were equilibrated overnight after sample collection before weighing for total mass.

In order to minimize the amount of blow-off and also allow losses to be checked, the sample line is cleaned ultrasonically with denatured ethyl alcohol. The sampler o-rings are inspected and replaced if needed. The base plate and slider are thoroughly cleaned and the system is mounted on the engine. Once the sampler is set up the engine is ready to be started.

The engine is then started. This is done using a hydraulic dynamometer which maintains a set speed of 1500 RPM. Once the engine is warmed up the timing and equivalence ratio were checked and set equal to 8° BTDC and 0.6 respectively. The engine coolant temperature was maintained at 82 °C.

Steady State

Once the engine was adjusted the dilution tunnel was turned on and its flow measurements taken. The exhaust was then piped into the dilution tunnel which was run

for 1 hour for conditioning, to come to "a particulate equilibrium". Once the tunnel was properly conditioned a 2 minute sample was taken from it using the MOUDI impactor. The tunnel dilution ratio was determined from measurements of the input air flowrate to the tunnel and engine air and fuel flowrates. Dilution ratios of 12 to 25 are provided by the tunnel depending on engine exhaust and dilution flows. The typical dilution ratio for these tests was 15.5.

Single Cycle

The components shown in figure 3.10 were used for these measurements. Groups of single cycle measurements were intermixed with steady state measurements as the engine continued to run. Before each measurement run, a conditioning run without the bag attached was made to remove easily suspended particulate matter from the base plate and sample line. The following processes are common to both conditioning and measurement runs: (i) The sampler quickly (in about 30 ms) moves the sample line in front of the exhaust port, (ii) the exhaust port opens and exhaust flows through the sample line, (iii) the exhaust valve closes, (iv) the sampler quickly returns to the rest position, and (v) the purge system discharges 10.5 standard liters of nitrogen through port B and the sample line. The purge nitrogen displaces residual exhaust from the valve and sample line. In a measurement run, the sample bag is connected to the sample line, the gate valve is opened, the sampler activated, and the gate valve is closed. The purge nitrogen introduced at the end of the sampler cycle forces exhaust remaining in port B and the sample line at the end of the exhaust stroke into the sample bag before the gate valve is closed. The bag was cleaned by flushing with nitrogen and filled with 141 standard liters

of nitrogen before each measurement run. At the end of each measurement run most of the contents of the sample bag were drawn through the MOUDI impactor/filter set for particle collection. A second, much smaller sample stream was drawn off for gas analysis. Concentrations of CO₂, NO, NO_x, and NO₂ are measured. The cylinder pressure, luminosity, needle lift, TDC, and sensor position were recorded on a digital oscilloscope for the measurement cycle and the cycle immediately preceding it. These data were downloaded to a personal computer for further analysis.

Dilution ratios were determined by taking the ratio of the standard volume of dilution nitrogen, sampling bag plus purge, to the standard volume of exhaust produced per engine cycle. The overall dilution ratio for these experiments was 260.

The foils and filters are weighed to determine the total (nonvolatile + volatile) particle mass, baked for 24 hours at 225 °C and re-weighed to determine the nonvolatile particle mass. The nonvolatile results are not presented here as the volatile fraction was within the range of the accuracy of the weighing method. Therefore, at the conditions measured there was essentially no difference between the total particle mass and the nonvolatile particle mass.

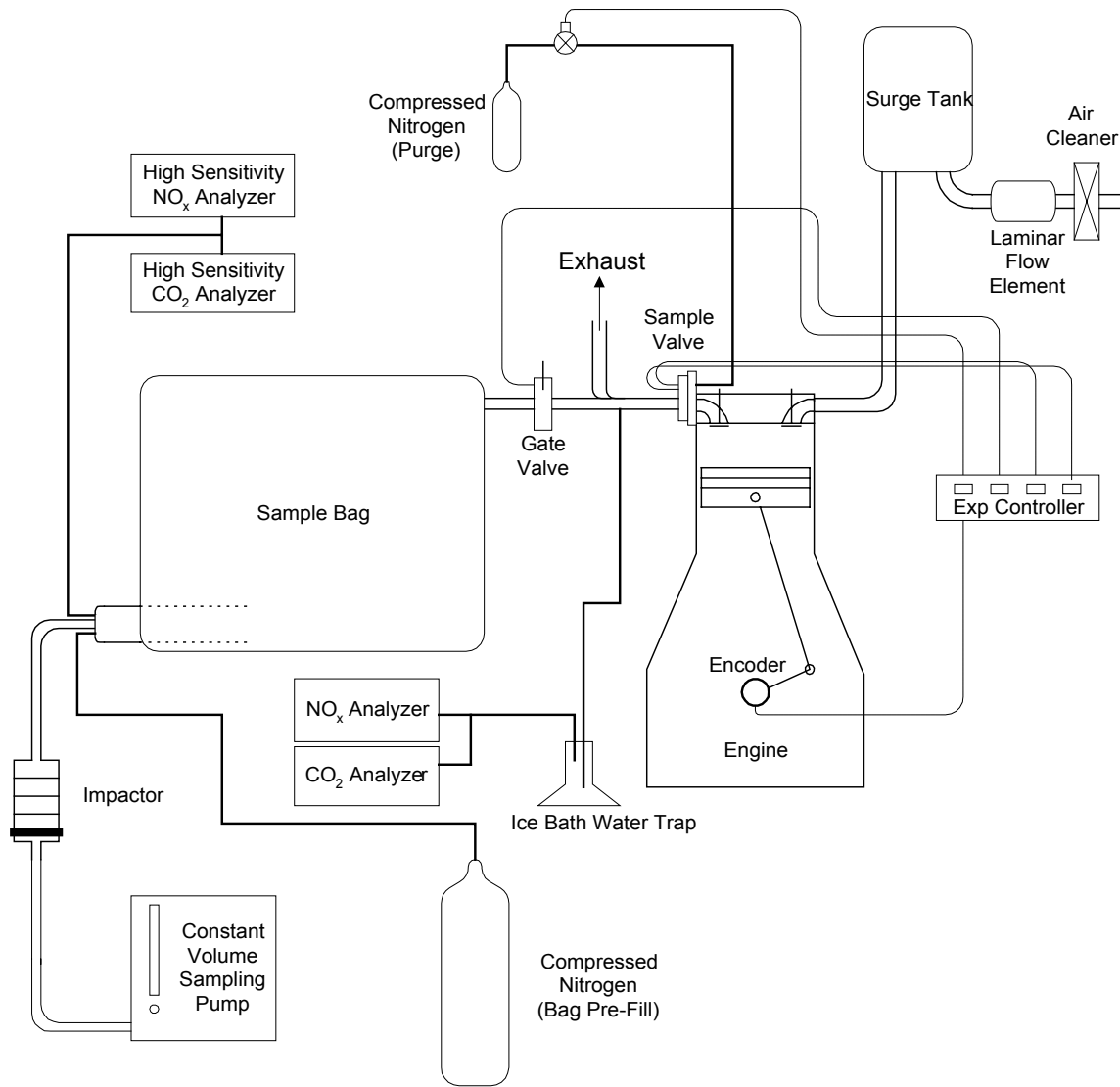


Figure 3.12 - Single Cycle Sampling Apparatus

4. Results & Discussion

A. Sampling System Performance

The performance of the sampling system was evaluated in two ways: first by determining the speed of the valve system, and second by evaluating leakage, particle losses, and particle resuspension in the system.

Speed of Response

The response was measured with the aforementioned apparatus. There is an approximately 20 ms delay from the time the control system sends the command to actuate a solenoid valve and the beginning of pressure rise in the pneumatic cylinder. This delay is not a problem because it remains essentially constant. It is accounted for in the control system by sending the move command approximately 20 ms (180 CAD at 1500 rpm) before the cylinder needs to start moving. Once pressure is applied to the pneumatic cylinder, another approximately 30 ms is required to move the valve from port to port. This performance is much better than the minimum requirement of 60 ms and allows sampling at speeds close to 3000 rpm. However, all tests described in this thesis were done at 1500 rpm. Figure 4.1 shows a representative plot of the photo-sensor output along with the in-cylinder pressure. The sample valve is moving when the sensor output is high and is in position when it is low. Exhaust Valve Open and Close are also indicated. As shown in figure 4.1 the sampler begins to move at 180 CAD before TDC

and is in position at 65 CAD after TDC. The exhaust valve doesn't open until 126 CAD after TDC at which time the valve is already in the sample position. The exhaust valve then closes at 386 CAD after TDC. Then the sampler moves to the rest, or normal exhaust, position from 540 to 805 CAD after TDC. The exhaust valve will open again at 1106 CAD ($386 + 720$) after the above TDC, at which time the exhaust is vented outside. From this it can be seen that the valve is able to move fast enough into position and back at the desired times.

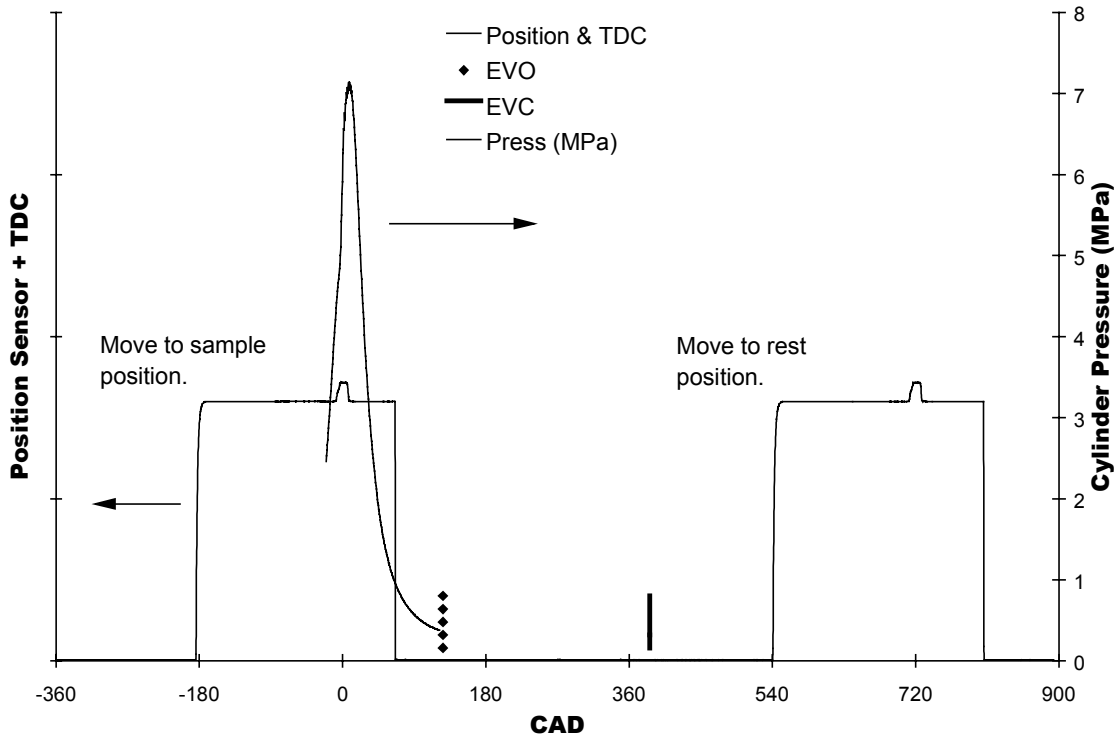


Figure 4.1 - Sample Valve Motion and Cylinder Pressure

Leakage, Particle Losses, and Resuspension

Sampling problems may lead to particle mass measurements that are erroneously high or low. Low measurements may result from particle losses in the valve and sampling system as well as from leakage. High measurements may result from: (I) resuspended particles -- particles deposited in the sampling system during prior cycles and then blown from the wall during the test cycle; (ii) debris -- wear and leakage related particles introduced into the sample flow by the movement of the sampling valve; and (iii) particles introduced into the sampling system directly by leakage of exhaust into the sample line while the engine is running with the exhaust in the exhaust line. Many experiments were performed to examine these problems. A series of preliminary tests were run before the nitrogen purge system was installed and cleaning procedures were established. Only filter samples were collected in these experiments. These tests gave only about 35 μg per cycle compared to an expected value, based on steady state measurements, of around 70-80 μg per cycle. It was then recognized that the volume of the sample line between port B and the sample bag was actually a larger than that of the exhaust produced each cycle, approximately 0.9 liters compared to the cylinder volume of 0.7 liters as indicated in figure 3.12. Most of the exhaust remaining in this part of the sampling system at the end of a test never reached the sample bag. After these preliminary single cycle sampling tests, the inside of the sampling line from the valve to the sample bag was examined. A significant amount of particulate matter was collected including carbon particles, aluminum filings, and paint. Part of this material was clearly associated with installation and initial operation, but much of the carbon apparently

resulted from particulate matter in the exhaust depositing on the sample line walls during and after the sampling cycle. The nitrogen purge system shown in Figure 3.7 was added to force all of the exhaust downstream of port B into the sampling bag. It discharges the contents of a 0.3 liter nitrogen cylinder charged to 3.4 MPa (10.5 standard liters) through port B and the sample line each time the sampler returns to its rest (non-sampling) position. The nitrogen is discharged into a small manifold where it enters the sample line through an orifice plate so that the entire line is swept clean.

After the purge system was installed, additional experiments were performed to examine sampling errors. The possibility of directly measuring particle losses in the sampling line by doing a series of experiments and then quantitatively determining the mass of particulate matter deposited on the inside of the sampling line was considered, but rejected as being too difficult and inaccurate. Instead sampling errors were examined by comparing size distributions and total masses measured for single cycle and steady state dilution tunnel exhaust samples. The size distribution measurements were made to help determine the role of resuspension in the sampling system. Most of the mass of freshly emitted diesel particulate matter is in the submicron diameter region, while resuspended particles are likely to be considerably larger. Thus the presence of larger particles might indicate resuspension. In any case a difference between size distributions of the exhaust particles and the particles from the single cycle sampler would indicate changes due to the sampling process. Similarly, differences between the average mass per cycle measured in the single cycle sampling experiments and that measured in steady state dilution tunnel experiments would indicate either sampling losses or gains.

The first size distribution measurements determined the mass of coarse particles, diameter $> 1 \mu\text{m}$, collected with the single cycle sampler. The MOUDI impactor equipped only with a $1 \mu\text{m}$ cut size stage was used for these measurements. The results are shown in the first two rows of table 4.1. Masses of 61 and 69 μg were measured in two runs. This was much more than expected. Usually only about 10% of the mass of diesel exhaust particulate matter is in particles larger than $1 \mu\text{m}$. The average mass per cycle determined from exhaust measurements was only about 80 μg . Thus, less than 10 μg of coarse particles were expected. More tests were done to examine this problem. In the next tests particles were collected on both impactor foils (diameter $> 1 \mu\text{m}$) and on backup filters (diameter $< 1 \mu\text{m}$). Both single cycle and steady state samples were taken. The results are also shown in table 4.1.

| bag filter (total mass) (μg) | bag foil (mass $> 1 \mu\text{m}$ dia.) (μg) | tunnel filter (total mass) ($\mu\text{g}/\text{cycle}$) | tunnel foil (mass $> 1 \mu\text{m}$ dia) ($\mu\text{g}/\text{cycle}$) |
|---|--|---|---|
| | 61 | | |
| | 69 | | |
| 157 | 143 | 88 | 11 |
| 135 | 69.5 | 114 | 9 |

The total mass collected per cycle with the single cycle sampler was more than twice that collected with the dilution tunnel. The difference is even more pronounced for the larger than $1 \mu\text{m}$ diameter particles collected on the impactor foils. The mass per

cycle collected on the foils with the single cycle sampler was more than ten times that collected from the dilution tunnel. This abnormally high concentration of coarse particles suggested that significant quantities of particles are being resuspended from surfaces within the sampling system.

The sample system was then disassembled and visually inspected for leaks. It appeared that particles were leaking into the sample line while it was in its rest position and the engine was running steadily. The o-rings appeared to allow a small exhaust flow to occur, from port A into port B, especially in regions where they were worn.

The next tests were designed to test how easy it was to resuspend particles from the walls of the valve and sampling line. The engine was run normally during the tests with the sampling valve in the exhaust (rest) position. Purge nitrogen was discharged through the sample line into the sampling bag at the end of the test period without moving the sampler from its rest position. Impactor foil and filter samples were collected from the bag. The results are shown in table 4.2. The amount of mass collected was small compared to that collected in the previous experiment. The first sample evidently gave higher results because it was the first test in the series and there was probably some particle mass on the base plate, around the o-rings, and in the sample line that was resuspended by the nitrogen purge. The masses determined in the second two experiments are not highly significant because the uncertainties in weighing foils and filters are 5-10 μg , i.e., in the same range as the observed masses.

| Table 4.2: Resuspension Testing Results | | | |
|---|---|--|-------|
| run time (min) | bag filter (total mass) (μg) | bag foil (mass > 1 μm dia.) (μg) | time |
| 8 | 17 | 13 | 11:45 |
| 30 | 6 | 7 | 12:15 |
| 7 | -4 | 1 | 12:22 |

The next test was to take a sample while the engine was running but on a non-fired cycle. While the engine was running steadily two consecutive fuel injection events were bypassed to produce two non-fired cycles. The single cycle sampler was activated on the second non-fired cycle. This allowed the amount of particulate mass blown from the walls during the sampling process to be estimated. The results are shown in table 4.3.

| Table 4.3: Non-fired Testing Results | | |
|---|--|----------------|
| bag filter (total mass) (μg) | bag foil (mass > 1 μm dia.) (μg) | time of sample |
| 56 | 163 | 1:33 |
| 11 | 24 | 1:45 |

Clearly mass was being blow from the walls of the sampling system. Both the samples had more than 2/3 of the particle mass in the coarse particle range. This is consistent with resuspension of particles from the walls of the system. Inspection of the base plate revealed evidence of leakage from the exhaust line onto the base plate.

Apparently this allowed deposits to build up around leakage points and around the interior of the o-ring. When the sampler was moved some of this mass was swept into the exhaust port and was subsequently blown into the sample line. For the first sample in table 4.3 the engine had been running for nearly 2 hours and more than an hour since the previous sample. The second sample was taken only twelve minutes after the first and the collected mass was much less. The collected mass is nearly directly proportional to the time from the last sample. This suggests that sampling cleans particles from the sampler surfaces and that a new deposit builds up linearly with time. After these tests the system was disassembled. There was visible leakage out of the exhaust line and an obvious buildup of soot on the base plate around the inside of the o-ring.

In order to ensure a "clean" system for the samples a conditioning run would be used to clean the base plate. A normal sampling event would be initiated with the sample bag removed from the end of the sample line. The bag would then quickly be attached and a normal sampling event performed.

Procedure to Minimize Sampling Artifacts

The experiments described above show that leakage and resuspension must be minimized for accurate sampling. Before beginning the test series described below the seals were carefully cleaned, adjusted, and replaced in necessary. In addition, a cleaning procedure was introduced to remove particles from sampling system surfaces before each test. A pre-sweep was used to clean the base plate. This was done by activating the single cycle sampler with the bag removed from the end of the sample line. The bag was then quickly reattached and the actual sample taken.

During the main tests described below, the sampler operated well. The move times stayed very consistent. Visual inspection showed no evidence of leakage.

B. Single Cycle Measurements

After the sampling procedure had been perfected, the main test series, which consisted of 25 single cycles, was run. Luminosity, total particle mass, NO_x, CO₂, fuel injection duration, and IMEP were measured on an individual basis. Three steady state tunnel measurements were also made during the test series. The test series took about 300 minutes to complete. Single cycle samples were taken at approximately ten minute intervals. The results of these measurements are summarized in table 4.4. The mean, maximum, minimum, standard deviation, and coefficient of deviation (standard deviation/mean) are given for each single cycle sampler data set. The results of the steady state tunnel measurements are also shown in Appendix 1. Some of the measurements, namely luminosity and particle mass, show considerable cycle-to-cycle variation. This is also apparent in figure 4.2 which is a plot of the variation of total particle mass, in mg per cycle, with elapsed time. Single cycle measurements show no clear trend in time but are more variable than the steady state tunnel measurements.

Table 4.5 summarizes the particle and NO_x measurements in terms of emission factors. Particle measurements made using the single cycle sampler give an emission factor 10% higher than the steady state tunnel measurements. This could indicate that some leakage and resuspension are occurring in the single cycle sampler. However, examination of the standard deviations of the results and a t-test, Appendix 2, suggest that the means are not significantly different. The emission factors observed are above the current standards, but

were measured at a low speed, high load condition that favors formation of both particles and NO_x. Measurements made following the Federal Test Procedure would presumably lead to much lower emission factors.

Figure 4.3 is a chart that illustrates the trend in variability in the data. The coefficients of variation (CV) for all the single cycle measurements are shown. Clearly

| Table 4.4: Summary Of Measurements* | | | | | | | |
|--|----------------|---------------|-----------------------------|-----------------------------|-----------------|--------------------|------|
| Single Cycle Sampler Measurements | | | | | | | |
| | PM (mg/cyc) | IMEP (MPa) | NO _x ** (ppm) | CO ₂ ** (ppm) | SOI*** (CAD) | Inj. Dur. (CAD) | Lum. |
| Mean | 0.087 | 0.76 | 3.89 | 319 | -8.26 | 16.6 | 0.16 |
| Max | 0.235 | 0.79 | 4.51 | 404 | -8.36 | 17.5 | 0.82 |
| Min | 0.021 | 0.74 | 3.2 | 273 | -8.04 | 16.3 | 0.02 |
| St Dev | 0.041 | 0.01 | 0.36 | 23.4 | 0.07 | 0.3 | 0.18 |
| C V | 0.48 | 0.02 | 0.09 | 0.07 | 0.01 | 0.02 | 1.09 |
| Steady State Measurements**** | | | | | | | |
| Tun | 0.079 | | 815 | 9.13 % | | | |
| Tun SD | 0.023 | | 40 | | | | |
| C V | 0.29 | | .05 | | | | |
| *All measurements made at 1500 rpm and a fuel-air equivalence ratio of 0.6 (full load). **Concentrations in sample bag. The overall dilution ratio from purge and bag nitrogen is 260 so exhaust concentrations are 260 times higher. ***SOI = Start of Injection ****Steady State NO _x and CO ₂ measurements are from a different day with similar operating conditions. | | | | | | | |

there are three groups: conventional combustion related quantities, injection duration, and IMEP, which have low CV's, gas related measurements, CO₂ and NO_x, which have medium CV's and particle related measurements, luminosity and particle mass, which have high CV's.

The low coefficients of variability, about 0.02, observed for the injection duration and IMEP show that in terms of typical measures the cycle-to-cycle variability is low. This is consistent with conventional wisdom about diesel engines.

The CO₂ and NO_x measurements gave CV's of 0.07 and 0.09 respectively. The amount of CO₂ produced per cycle is directly proportional to the amount of fuel injected, which is in turn proportional to the injection duration. The greater variability observed for CO₂ compared to injection duration is due to inconsistencies in the single cycle sampler and uncertainties in the CO₂ measurements. The repeatability of the high sensitivity CO₂ analyzer used for these measurements is no better than about 5%. It is assumed that the errors combine following the mean square error law²⁴, i.e.,

$$\delta_{overall} = \sqrt{(\delta^2_{CO_2} + \delta^2_{fuel} + \delta^2_{sampler})}$$

where δ is the fractional error and the subscripts overall, CO₂, fuel, and sampler denote the overall error, errors introduced by the CO₂ measurement, fuel injection quantity, and single cycle sampler, respectively. If it is assumed the δ_{fuel} is equal to the CV for injection duration and $\delta_{overall}$ is equal to the CV for single cycle sampler CO₂ measurements, one can solve for $\delta_{sampler}$. This gives a sampler uncertainty of only about 4%.

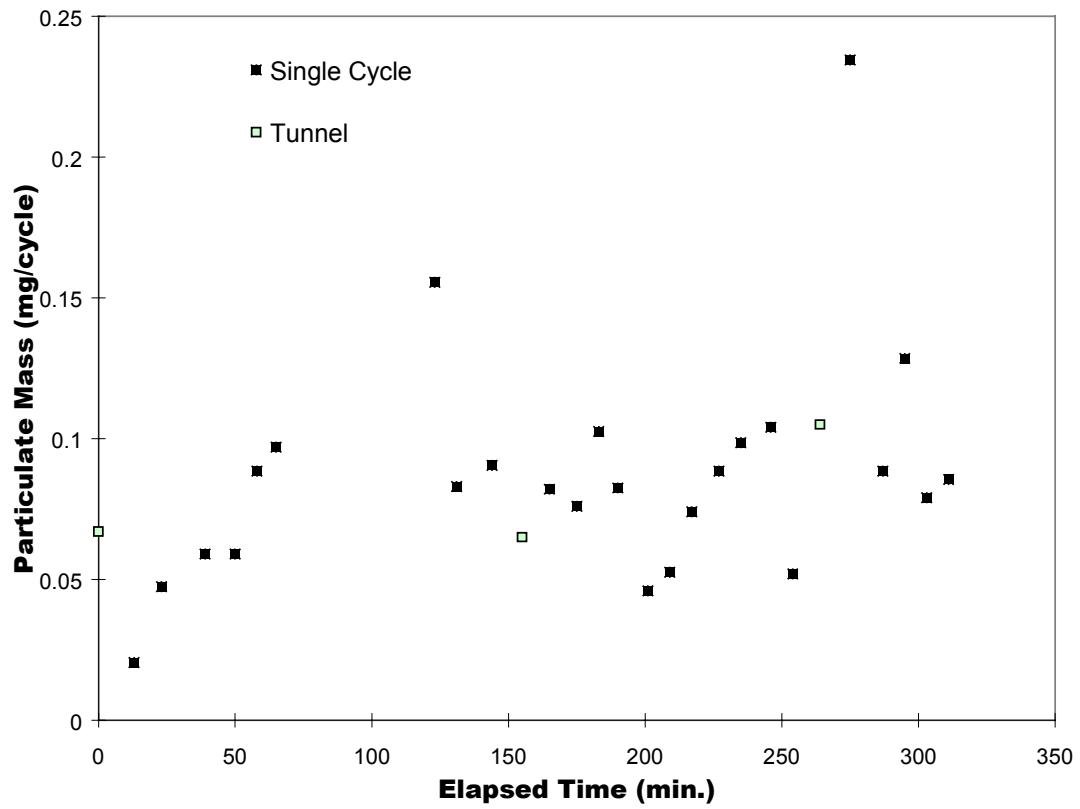


Figure 4.2 - Total Particle Mass Emissions

| Table 4.5: Brake Specific Emissions* | | |
|---|------------------------------|--------------------------------|
| | Particle Mass (gm/ihp-hr) | NO _x (gm/ihp-hr) |
| Single Cycle Sampler Measurements | | |
| Mean | 0.44 | 5.87 |
| St Dev of Mean | 0.04 | 0.11 |
| Steady State Tunnel Measurements | | |
| Mean | 0.40 | 4.73 |
| St Dev of Mean | 0.07 | 0.13 |
| *All measurements made at 1500 rpm and a fuel-air equivalence ratio of 0.6 (full load). | | |

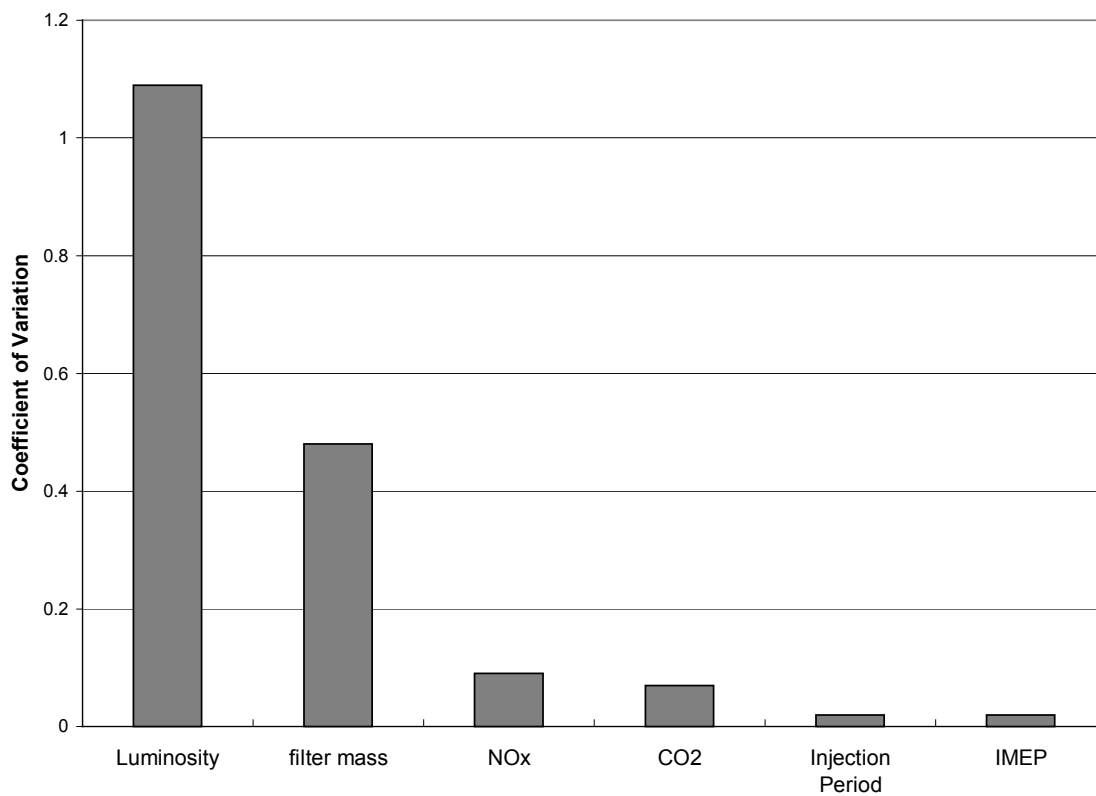


Figure 4.3 - Coefficients of Variation for Single Cycle Sampler Measurements

The same approach may be used to find the cyclic variability in NO_x formation.

Thus:

$$\delta_{overall_NO_x} = \sqrt{(\delta_{sampler}^2 + \delta_{NO_x}^2 + \delta_{NO_x_instrument}^2)}$$

The NO_x instrument uncertainty is about 5%. Solving for the inherent cyclic variability in the formation of NO_x give 6%. This shows that NO_x formation has a higher order dependence on details of the combustion process than do the overall combustion parameters like IMEP.

The particle related measurements show by far the greatest level of cyclic variability. The luminosity has a coefficient of variation over 1. This very high variability is due to several factors. The luminosity sensor measures the infrared radiation from the flame that is in front of the sensor window. The signals shown are averages over the 33-38 CAD window. This window was taken because it was near the end of the combustion process and gave a fairly consistent and large signal. Even this signal was highly variable, presumably as a result of variations in the flame position, particle concentration, temperature, and deposition and resuspension of particles on the sensor window. The luminosity signal degenerated significantly during the course of the study making the measurements somewhat suspect. The reason that the luminosity measurements were included in these experiments is that it was hoped that the late cycle luminosity would correlate with the particle mass emitted on a given cycle. No such correlation was found. Because of this and the difficulties in the interpretation of this signal, no further analysis of luminosity was attempted.

The single cycle particle mass measurements were the primary objective of this study. They show a high degree of variability with a CV of 0.48. In order to find the variability attributed to the in-cylinder processes, sources of error in this measurement must be considered. Using the root mean square error approach gives:

$$\delta_{overall} = \sqrt{(\delta_{sampler}^2 + \delta_{filter}^2 + \delta_{sampler_p}^2 + \delta_{in_cylinder}^2)}$$

here:

$\delta_{overall}$ is 0.48, the coefficient of variability for the measured particle mass.

$\delta_{sampler}$ is 0.04, the error in the sampling efficiency determined for the CO₂ measurement.

δ_{filter} is the error in determination of the particle mass associated with weighing the filter and impactor foils. The mean particle mass was 87 µg, and the weighing uncertainty was 10 µg. Thus the fractional error is 0.11.

$\delta_{sampler_p}$ is the error associated with particle leakage and resuspension in the sampler. On the basis of the system performance experiments described above, the mass uncertainty is estimated to be 20 µg. This gives a fractional uncertainty of 0.23.

$\delta_{in-cylinder}$ is the variability associated with actual in-cylinder processes to be determined.

Solving for the in-cylinder variability gives a value of 0.40. Thus even when all the sources of sampling error are accounted for, a large cyclic variability of particle mass emissions is indicated.

C. Steady State Measurements

The coefficient of variability for the steady state sampling system can also be determined using the root mean square error approach as follows:

$$\delta_{overall_SS} = \sqrt{(\delta_{filter_SS}^2 + \delta_{sampling_SS}^2 + \delta_{engine_SS}^2)}$$

here:

$\delta_{overall_SS}$ is 0.29, the coefficient of variability for the measured particle mass.

$\delta_{sampling_SS}$ is 0.02, the error in the sampling due to possible leaks.

δ_{filter_SS} is the error in determination of the particle mass associated with weighing the filter and impactor foils. The mean particle mass was 79 μg , and the weighing uncertainty was 10 μg . Thus the fractional error is 0.13.

δ_{engine_SS} is the variability associated with in-cylinder processes to be determined as measured by the steady state system. Solving for the in-cylinder variability gives a value of 0.26. This is slightly more than half the variability seen by the single cycle sampler and is consistent with the expected results. A steady state measurement system would tend to average out any variability present in the engine and lead to more stable particle mass measurements.

D. Discussion of Single Cycle Tests

The results of these experiments show that NO_x and particle emissions from a diesel engine are subject to significant cyclic variability. Attempts to model NO_x and particle emissions from an indirect diesel engine^{13,14} have shown that NO_x emissions are more sensitive and particle emissions are much more sensitive to combustion parameters

than is the IMEP. This is consistent with the pattern of variability observed in these experiments. An attempt was made to establish a relationship between cycle-to-cycle changes in the variables measured. The resulting correlation coefficients are shown in table 4.6. All the correlation's are weak as the generally accepted range for a strong correlation is between 0.8 and 1, absolute value. The largest coefficient is seen between filter mass (particulate) and NO_x. It is generally accepted that these parameters exhibit an inverse relationship in diesel engines which is what the negative coefficient shows. The next largest coefficient is between injection duration and IMEP, that is, more fuel leads to more power. The other coefficients tend to be even less significant.

| | PM | IMEP | NO _x | CO ₂ | SOI | Inj. Dur. | Lum. |
|-----------------|---------|---------|-----------------|-----------------|---------|-----------|------|
| PM | -- | -- | -- | -- | -- | -- | -- |
| IMEP | -0.3171 | -- | -- | -- | -- | -- | -- |
| NO _x | -0.4984 | 0.3162 | -- | -- | -- | -- | -- |
| CO ₂ | 0.0901 | 0.0449 | 0.3243 | -- | -- | -- | -- |
| SOI | -0.0487 | 0.0865 | 0.2502 | -0.1014 | -- | -- | -- |
| Inj. Dur. | 0.3328 | 0.4260 | -0.3575 | 0.0611 | -0.0530 | -- | -- |
| Lum. | 0.1375 | 0.03286 | -0.18475 | 0.1097 | -0.1870 | 0.2706 | -- |

In order to gain additional insights into the nature of the observed cyclic variability, some of the results have been plotted in the form of cumulative distributions. Figure 4.4 shows cumulative frequency distributions for the IMEP, NO_x, and particle mass measurements. The distributions give the fraction of cycles producing less than the value indicated on the ordinate. Ordinate values are normalized by dividing the mean so that all values may be plotted on the same scale, e.g., for IMEP, $IMEP/IMEP_{mean}$ is used. The plots again show the significant variability of the particle measurements. Associated with this variability is the fact that a significant fraction of the cycles produce particle emissions well below the mean value. It is interesting to consider what might lead to these low emission cycles. One explanation is that the particle formation and oxidation processes are highly sensitive to details of the combustion process and the right conditions exist to produce these low emission cycles a significant fraction of the time. If so, these conditions should be identified. An alternative explanation is deposition/resuspension. Several recent papers^{8,15,9} have measured rates of deposition and or resuspension of particles on in-cylinder surfaces of diesel engines. These studies suggest that a significant fraction, 25% or more, of the particulate matter emitted from diesel engines has been deposited on in-cylinder surfaces and subsequently been resuspended. This mechanism is completely consistent with the observed cyclic variability of particulate emissions seen in this study. If this is the source of the variability, the low emitting cycles are those in which very little material is resuspended, while the high ones are those in which a large quantity of material is resuspended.

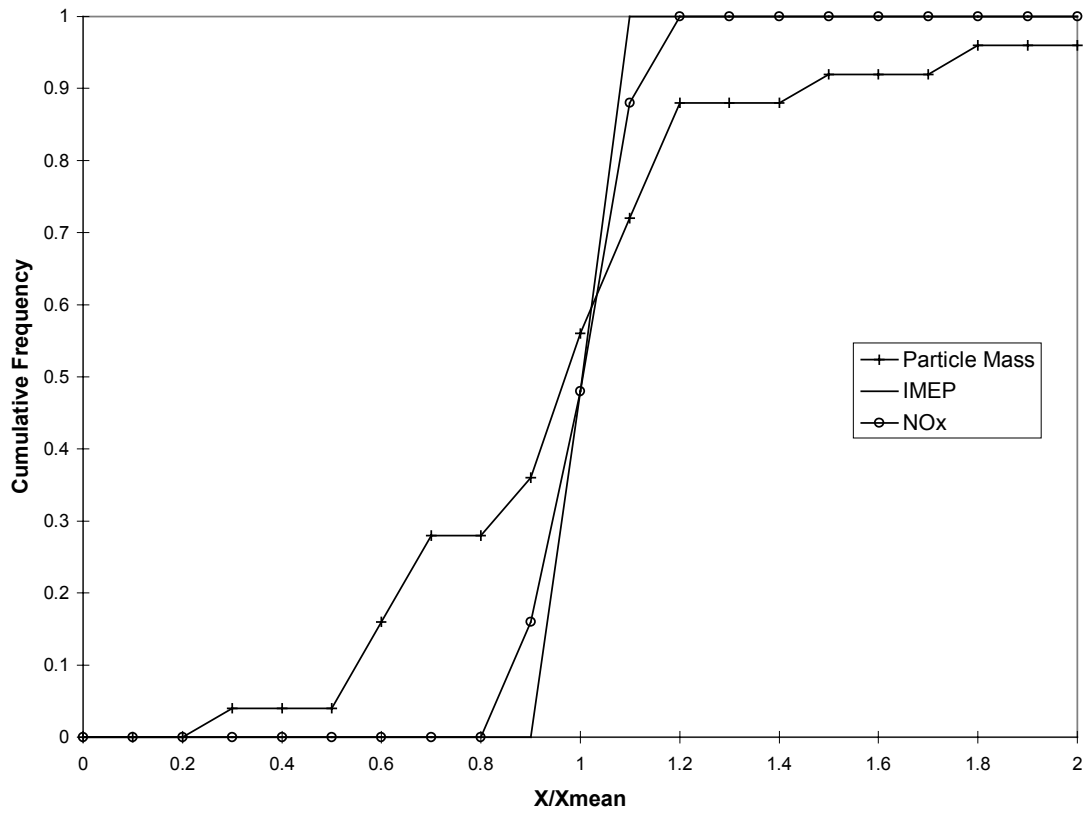


Figure 4.4 - Cumulative Frequency Distributions for Single Cycle Measurements

5. Conclusions & Recommendations

The single cycle sampler designed for this study performed well for measurements of both gaseous and particulate emissions. Before applying it to engine measurements, the system was analyzed for sources of variability generated by the system itself, rather than the engine. The sampler operated well in that the move times stayed very consistent and a visual inspection showed losses to be almost nonexistent. As to the question of gains from a possible leak from the exhaust line into the sample line a visual inspection here showed no sign of such a leak. This leaves the port volume as one variable, along with particle deposition and reentrainment from within the sample line.

The sampler was used to study the cyclic variability of a 0.7 liter direct injection diesel cylinder operating at 1500 rpm and an equivalence ratio of 0.6. Particulate emissions exhibited the greatest variability. The cyclic variability (standard deviation) of particulate emissions associated with in-cylinder processes was found to be about 40% of the mean. The variability of NO_x emissions that could be associated with in-cylinder processes was much lower, only about 6% of the mean. The variability of the pressure development in the combustion process itself, as indicated by IMEP, was very low, less than 2% of the mean. The high variability of particulate emissions may be due to high sensitivity of the formation/oxidation balance to small changes in the combustion process, to in-cylinder surface deposition/resuspension processes, to some combination of the two, or to some other unidentified phenomenon.

This work adds to a growing body of evidence that in-cylinder surfaces play an important role in determining particulate emissions from diesel engines. If surfaces are important, they may act as reservoirs that store particulate matter, protect it from oxidation, and ultimately reemit it in a somewhat random manner. In that case, combustion systems that minimize particle formation early in the combustion process, do not rely on late cycle oxidation, and keep particle formation away from walls might have very low particulate emissions. Furthermore, if surfaces are important, appropriate surface coatings might significantly influence particulate emissions.

This work raises some interesting questions, but it was done on only one engine, at one operating condition, and with a new sampling technique. Additional work should be done on other engines and at other operating conditions. More validation experiments should be done on the sampler and non-intrusive optical methods for single cycle emission measurements should be investigated further.

For system upgrades; the Nitrogen purge line should be moved to the exhaust port as near the valve as possible as done by Ferguson³ and the flexible stainless steel lines could be replaced with a silicone impregnated fiberglass line as was done by Stenerson.¹

Bibliography

1. Stenerson, E., "Cyclic Variability of Emissions from a Diesel Engine", M.S. Thesis, University of Minnesota, Minneapolis, Minnesota, (1995).
2. Xu, H., P.S. Meyers, and O.A. Uyehara, "In Cylinder Measurement of Particulate Number Density and Size", SAE paper no. 820462, (1982).
3. Ferguson, C.R., M Chapman, H. Kizawa, and R.F. Nash, "Diesel Exhaust Opacity: At the Port and a Meter Downstream", SAE paper no. 831724, (1983).
4. Kittelson, D.B. and N. Collings, "Origin of the Response of Electrostatic Particle Probes", SAE paper no. 870476, 1987 Transactions of the SAE (1988).
5. Pipho, M.J., J.A. Ambs, and D.B. Kittelson, "In-Cylinder Measurements of Particulate Formation in an Indirect Injection Diesel Engine", SAE paper no. 860024, (1986).
6. Kittelson, D.B., M.J. Pipho, J.L. Ambs, and L. Luo, "In-Cylinder Measurements of Soot Production in a Direct-Injection Diesel Engine", SAE paper no. 880344, 1988 Transactions of the SAE (1989).
7. Yan, J. and G.L. Borman, "Analysis and In-Cylinder Measurement of Particulate Radiant Emissions and Temperature in a Direct Injection Diesel Engine", SAE paper no. 881315, (1988).
8. Kittelson, D.B., J.L. Ambs, and H. Hadjkacem, "Particulate Emissions from Diesel Engines: Influence of In-Cylinder Surface", presented at the SAE International Congress and Exposition, Detroit, MI, February 26-March 2, 1990, SAE paper no. 900645, 1990 Transactions of the SAE, J. of Engines, Vol. 99, Sec. 3 (1991).
9. Abukdais, M., "Time Resolved Exhaust Sampling from an Indirect Injection Diesel Engine", Ph.D. Thesis, University of Minnesota, Minneapolis, Minnesota, (1991).
10. Pipho, M.J., "Total Cylinder Sampling from a Diesel Engine", Ph.D. Thesis, University of Minnesota, Minneapolis, Minnesota, (1990).
11. Marple, V.A., K.L. Rubow, and Steven M. Behm, "A Microorifice Uniform Deposition Impactor (MOUDI)", Aerosol Sci. Technol., 14, pp. 434-446, (1991).

12. Rubow, K.L., Private Communication, Particle Technology Laboratory, University of Minnesota, Minneapolis, Minnesota, (1992).
13. Liu, X.J., D. Siegl, and D.B. Kittelson, "In-Cylinder NO_x Histories in an Indirect Injection Diesel Engine: Comparisons Between Experimental Data and Model Predictions", presented at the Colloquium on Engine Combustion, 20th International Symposium on Combustion, Ann Arbor, MI (August 12-17, 1984).
14. Kittelson, D.B., M.J. Piphon, J.L. Ambs, and D.C. Siegl, "Particle Concentrations in a Diesel Cylinder: Comparison of Theory and Experiment", SAE paper no. 861569, 1986 Transactions of the SAE (1987).
15. Hadjkacem, H., "Time Resolved Measurements of Particulate Matter in Diesel Exhaust", M.S. Thesis, University of Minnesota, Minneapolis, Minnesota, (1990).
16. Takeuchi, K., K. Kubota, M. Konagi, M. Watanabe, and R Kihara, "The New Isuzu 2.5 Liter and 2.8 Liter 4-Cylinder Direct Injection Diesel Engine", SAE paper no. 850261, 1985.
17. Sinnamon, J.F., D.R. Lancaster, and J.C. Stiener, "An Experimental and Analytical Study of Engine Fuel Spray Trajectories", SAE paper no 800135, 1980.
18. Bartok, W. & A.F. Sarofim, Fossil Fuel Combustion, A Source Book, Wiley-Interscience
19. Heywood, J.B. Internal Combustion Engine Fundamentals, McGraw-Hill
20. Tree, D.R. & D.E. Foster, "Optical Measurements of Soot Particle Size, Number Density, and Temperature in a Direct Injection Diesel Engine as a Function of Speed and Load", SAE paper no 940270, 1994.
21. Yamaguchi, H., H. Tanabe, and G. T. Sato, "A Study of Particulate Formation on the Combustion Chamber Wall", SAE paper no 910488, 1991.
22. Holman, J.P., & W.J. Gajda, Jr., Experimental Methods for Engineers, Fifth Edition, McGraw-Hill

Appendix 1: Summarized Data

| Measurement Data and Summary Statistics | | | | | | | | | |
|---|------------------|------------------|------------|---------------------------|---------------------------|-----------|-----------------|-------------------|------------------|
| Filter | elpsd time (min) | filter mass (μg) | IMEP (MPa) | NO _x AVG (ppm) | CO ₂ AVG (ppm) | SOI (CAD) | inj. dur. (CAD) | Lum. avg. (33-38) | tunnel mass (μg) |
| T101 | 0 | | | | | | | | 0.067 |
| 102 | 13 | 0.0205 | 0.769 | 3.89 | 273.46 | -8.26 | 16.724 | 0.092 | |
| 103 | 23 | 0.0475 | 0.773 | 4.51 | 324.35 | -8.27 | 16.386 | 0.2345 | |
| 104 | 39 | 0.059 | 0.765 | 4.25 | 310.58 | -8.04 | 16.402 | 0.047 | |
| 105 | 50 | 0.059 | 0.768 | 4.23 | 304.77 | -8.36 | 16.425 | 0.074 | |
| 106 | 58 | 0.0885 | 0.759 | 3.77 | 316.46 | -8.26 | 16.547 | 0.8215 | |
| 107 | 65 | 0.097 | 0.749 | 3.49 | 307.65 | -8.32 | 16.305 | 0.1365 | |
| 108 | 123 | 0.1555 | 0.745 | 3.20 | 287.30 | -8.27 | 16.43 | 0.2 | |
| 109 | 131 | 0.083 | 0.756 | 4.21 | 403.90 | -8.34 | 16.375 | 0.1925 | |
| 110 | 144 | 0.0905 | 0.758 | 4.41 | 324.90 | -8.32 | 16.475 | 0.327 | |
| T111 | 155 | | | | | | | | 0.065 |
| 112 | 165 | 0.082 | 0.759 | 3.64 | 332.58 | -8.27 | 16.402 | 0.035 | |
| 113 | 175 | 0.076 | 0.771 | 4.33 | 332.91 | -8.25 | 16.481 | 0.044 | |
| 114 | 183 | 0.1025 | 0.744 | 4.07 | 309.43 | -8.25 | 16.612 | 0.082 | |
| 115 | 190 | 0.0825 | 0.75 | 3.70 | 317.43 | -8.30 | 16.62 | 0.042 | |
| 116 | 201 | 0.046 | 0.747 | 3.94 | 317.10 | -8.23 | 16.347 | 0.0255 | |
| 117 | 209 | 0.0525 | 0.756 | 3.63 | 296.98 | -8.26 | 16.369 | 0.016 | |
| 118 | 217 | 0.074 | 0.762 | 3.95 | 314.92 | -8.24 | 16.509 | 0.07 | |
| 119 | 227 | 0.0885 | 0.773 | 3.32 | 329.79 | -8.26 | 17.487 | 0.488 | |
| 120 | 235 | 0.0985 | 0.771 | 4.16 | 347.42 | -8.24 | 17.079 | 0.0605 | |
| 121 | 246 | 0.104 | 0.77 | 3.91 | 332.54 | -8.24 | 16.915 | 0.24 | |
| 122 | 254 | 0.052 | 0.785 | 4.05 | 319.69 | -8.24 | 16.823 | 0.1735 | |
| T123 | 264 | | | | | | | | 0.105 |
| 124 | 275 | 0.2345 | 0.751 | 3.24 | 318.13 | -8.3 | 17.108 | 0.1845 | |
| 125 | 287 | 0.0885 | 0.776 | 3.63 | 316.35 | -8.33 | 16.995 | 0.217 | |
| 126 | 295 | 0.1285 | 0.773 | 4.18 | 323.95 | -8.08 | 16.625 | 0.0485 | |
| 127 | 303 | 0.079 | 0.776 | 3.85 | 308.87 | -8.29 | 16.792 | 0.0745 | |
| 128 | 311 | 0.0855 | 0.785 | 3.83 | 305.74 | -8.31 | 16.744 | 0.101 | |
| | | | | | | | | | |
| MIN | | 0.0205 | 0.744 | 3.20 | 273.46 | -8.36 | 16.305 | 0.016 | |
| MAX | | 0.2345 | 0.785 | 4.51 | 403.90 | -8.04 | 17.487 | 0.8215 | |
| AVG | | 0.087 | 0.764 | 3.89 | 319.09 | -8.26 | 16.648 | 0.161 | 0.079 |
| STDEV | | 0.041 | 0.012 | 0.35 | 22.948 | 0.07 | 0.289 | 0.173 | 0.018 |

Appendix 2: t-test results

| bag filter mass | tunnel filter mass |
|-----------------|--------------------|
| 0.0205 | 0.067 |
| 0.0475 | 0.065 |
| 0.059 | 0.105 |
| 0.059 | |
| 0.0885 | |
| 0.097 | |
| 0.1555 | |
| 0.083 | |
| 0.0905 | |
| 0.082 | |
| 0.076 | |
| 0.1025 | |
| 0.0825 | |
| 0.046 | |
| 0.0525 | |
| 0.074 | |
| 0.0885 | |
| 0.0985 | |
| 0.104 | |
| 0.052 | |
| 0.2345 | |
| 0.0885 | |
| 0.1285 | |
| 0.079 | |
| 0.0855 | |

| t-Test: Two-Sample Assuming Unequal Variances | | |
|---|-------------------|-------------------|
| | <i>Variable 1</i> | <i>Variable 2</i> |
| Mean | 0.087 | 0.079 |
| Variance | 0.001709 | 0.000508 |
| Observations | 25 | 3 |
| Hypothesized Mean Difference | 0 | |
| df | 4 | |
| t Stat | 0.518898 | |
| P(T<=t) one-tail | 0.315609 | |
| t Critical one-tail | 2.131846 | |
| P(T<=t) two-tail | 0.631218 | |
| t Critical two-tail | 2.776451 | |